INFORMATION CLEARANCE REVIEW AND RELEASE APPROVAL

Part I: Background Information

Title:	Information Category:
Solid Phase Characterization of Tank 241-C-105 Grab Samples	☐ Abstract ☐ Journal Article ☐ Summary ☐ Internet ☐ Visual Aid ☐ Software ☐ Full Paper ☒ Report ☐ Other
Publish to OSTI? ☒ Yes ☐ No	

Document Number: LAB-RPT-15-00011 Date: 12/17/15 JRR 1/11/2016

Author: T. M. Ely, M. E. LaMothe and J. S. Lachut

Purpose of Document: Report on Sample Analysis

Part II: External/Public Presentation Information

Conference Name: N/A

Sponsoring Organization(s):

Date of Conference:	Conference Location:

Will Material be Handed Out? ☐ Yes ☐ No Will Information be Published? ☐ Yes ☐ No *(If Yes, attach copy of Conference format instructions/guidance.)*

Part III: WRPS Document Originator Checklist

Description	*Yes*	*N/A*	*Signature*
Information Product meets requirements in TFC-BSM-AD-C-01?	☐	☒	
Document Release Criteria in TFC-ENG-DESIGN-C-25 completed? (Attach checklist)	☐	☒	
If product contains pictures, safety review completed?	☒	☐	Robin Fogg Robin Fogg 12/17/15

Part IV: WRPS Internal Review

Function	*Organization*	*Date*	*Print Name/Signature/Date*
Subject Matter Expert	Process Chemistry	12-17-15	TOM ELY Tom Ely 12-17-15
Responsible Manager	Process Chemistry	12-17-15	CARY A. Cook Cary A. Cook 12/17/15
Other: J.M. Frye	WRPS	01-07-16	Approved via IDMS data file.

Part V: IRM Clearance Services Review

Description	*Yes*	*No*	*Print Name/Signature*
Document Contains Classified Information?	☐	☑	If Answer is "Yes," ADC Approval Required Print Name/Signature/Date
Document Contains Information Restricted by DOE Operational Security Guidelines?	☐	☑	Reviewer Signature: Print Name/Signature/Date
Document is Subject to Release Restrictions? *If the answer is "Yes," please mark category at right and describe limitation or responsible organization below:*	☐	☑	Document contains: ☐ Applied Technology ☐ Protected CRADA ☐ Personal/Private ☐ Export Controlled ☐ Proprietary ☐ Procurement – Sensitive ☐ Patentable Info. ☐ Business - Sensitive ☐ Predecisional Info. ☐ UNCNI ☐ Restricted by Operational Security Guidelines ☐ Other (Specify)
Additional Comments from Information Clearance Specialist Review?	☐	☑	Information Clearance Specialist Approval APPROVED By Julia Raymer at 10:47 am, Jan 11, 2016 Print Name/Signature/Date

When IRM Clearance Review is Complete – Return to WRPS Originator for Final Signature Routing (Part VI)

Part VI: Final Review and Approvals

INFORMATION CLEARANCE REVIEW AND RELEASE APPROVAL

Description	Approved for Release		Print Name/Signature
	Yes	N/A	
WRPS External Affairs	☐	☑	
WRPS Office of Chief Counsel	☐	☑	
DOE – ORP Public Affairs/Communications	☐	☑	
Other:	☐	☐	
Other:	☐	☐	

Comments:

APPROVED
By Julia Raymer at 10:48 am, Jan 11, 2016

Approved for Public Release;
Further Dissemination Unlimited

Information Release Station

Was/Is Information Product Approved for Release? ☑ Yes ☐ No

If Yes, what is the Level of Releaser? ☑ Public/Unrestricted ☐ Other (Specify) _____

Date Information Product Stamped/Marked for Release: 1/11/16

Was/Is Information Product Transferred to OSTI? ☑ Yes ☐ No

Forward Copies of Completed Form to WRPS Originator and WRPS CIO Office

Description	Yes	N/A	Print Name/Signature
WRPS Information Product	☐	☐	
Conference Paper Guidelines	☐	☐	
Trademark/Copyright "Right to Use" Information or Permission Documentation	☐	☐	
WRPS Administrative Checklist	☐	☐	
	☐	☐	
	☐	☐	

Solid Phase Characterization of Tank 241-C-105 Grab Samples

T. M. Ely
M. E. LaMothe
J. S. Lachut

Washington River Protection Solutions LLC

Date Published
December 2015

Prepared for the U.S. Department of Energy
Office of River Protection

Contract No. DE-AC27-08RV14800

TRADEMARK DISCLAIMER

Reference herein to any specific commercial product, process, or service by tradename, trademark, manufacturer, or otherwise, does not necessarily constitute or imply its endorsement, recommendation, or favoring by the United States Government or any agency thereof or its contractors or subcontractors.

Printed in the United States of America

Total pages: 32

Table of Contents

List of Tables

List of Figures

List of Terms

Acronyms and Abbreviations

C-105	Tank 241-C-105
EDS	energy dispersive spectrometry
ICDD PDF4+	International Center for Diffraction Data Powder Diffraction File 4+
MDI	Materials Data Incorporated
PLM	polarized light microscopy
SEM	scanning electron microscopy
SPC	solid phase characterization
XRD	X-ray diffraction

Units

g	gram
mL	milliliter
µm	micrometer

1 INTRODUCTION

The solid phase characterization (SPC) of three grab samples from single-shell Tank 241-C-105 (C-105) that were received at the laboratory the week of October 26, 2015, has been completed.

The three samples were received and broken down in the 11A hot cells. The sample identification and amounts are as shown in Table 1.

Table 1. Sample Identification, Sample Identification in OmniLIMS[1], Volume, and Weight.

Sample ID	OmniLIMS #	Approximate Volume (mL)	Approximate Amount (g)
105C-15-01	S15T023591	120	92.0
105C-15-02	S15T023603	150	116.3
105C-15-03	S15T023614	120	113.4

The photos in Figure 1 were taken through the hot cell window and have been cropped and brightened considerably:

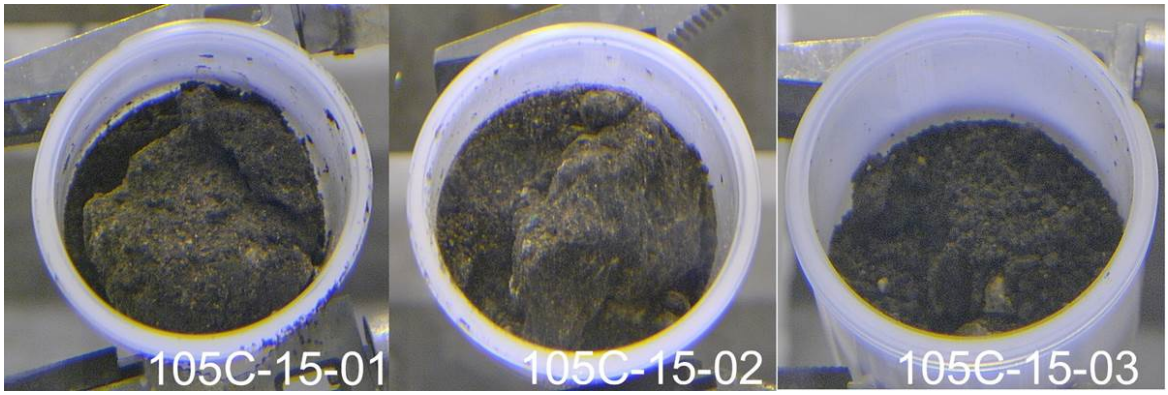

Figure 1. Photos of Three Tank 241-C-105 Samples Taken Through the Hot Cell Window.

The color of the recovered material is generally dark brown to black. Some white grains were visible, and an indurated piece from 105C-15-03 was a lighter tan color. Subsamples for SPC were taken as follows: 105C-15-01 (S15R000622), 105C-15-02 (S15R000623), 105C-15-03 dark grains (S15R000624), 105C-15-03 tan aggregate (S15R000625). 105C-15-03 was subsampled prior to homogenization so that the large tan aggregate visible in Figure 2 could be

[1] OmniLIMS is a trademark of Columbia Energy and Environmental Services, Richland, Washington.

sub-sampled. It crushed with some difficulty, while the darker aggregates in this sample, as well as the dark aggregates in the first two samples, broke apart more easily.

Figure 2. Photo of 105C-15-3, Through the Hot Cell Window, Showing Large Tan Aggregate Subsampled for Analysis.

Analysis by SPC at the 222-S Laboratory consists primarily of X-ray diffraction (XRD), polarized light microscopy (PLM), and scanning electron microscopy (SEM).

Subsamples for SEM analysis were prepared by crushing sample splits further. Several large pieces of the white aggregate were affixed to SEM stubs using carbon-based glue. The other samples were prepared by dispersing and crushing the larger aggregates and lifting the particulates with an SEM stub covered with an adhesive carbon tape. Subsamples for PLM analysis were prepared by mounting in index oil, or with the addition of a drop of water.

2 X-RAY DIFFRACTION

2.1 SAMPLE PREPARATION

Small amounts of solid sample material were added to a miniature mortar and then ethyl alcohol was added to cover the solids. The solids were subsequently ground to a flourlike consistency and left in the mortar until all of the alcohol evaporated, leaving the powder residue completely dry. The powder solids were disbursed on a single crystal silicon substrate coated with a thin layer of petroleum jelly. Loose powder particles were removed by inverting the substrate and tapping on the reverse side of the substrate. The powder deposits were inspected for uniformity of the deposit, and additional powder was deposited as needed until a uniform deposit was achieved. The coated substrate was installed in an aluminum sample support designed to

interface with the autosample changer on the Rigaku™[2] MiniFlex II. The sample cup was installed in the diffractometer, and measurements were performed in accord with ATS-LT-507-103, "222-S Laboratory X-Ray Diffractometry (XRD) Using the Rigaku MiniFlex II."

2.2 DATA PROCESSING

Background Subtraction: Raw data was processed using MDI Jade software in conjunction with the International Center for Diffraction Data Powder Diffraction file version 4+ (ICDD PDF4+) diffraction data database. In general, each pattern was background subtracted prior to further processing. The amorphous contribution of the petroleum jelly layer was accounted for by overlaying a diffraction pattern from pure petroleum jelly on sample data. The petroleum jelly pattern was scaled to match the sample data; background points were then specified on the sample data, and the background level in the sample data was eliminated (see Figure 3). Two crystalline peaks associated with the petroleum jelly adherent layer were also manually subtracted from each data set prior to phase identification analysis.

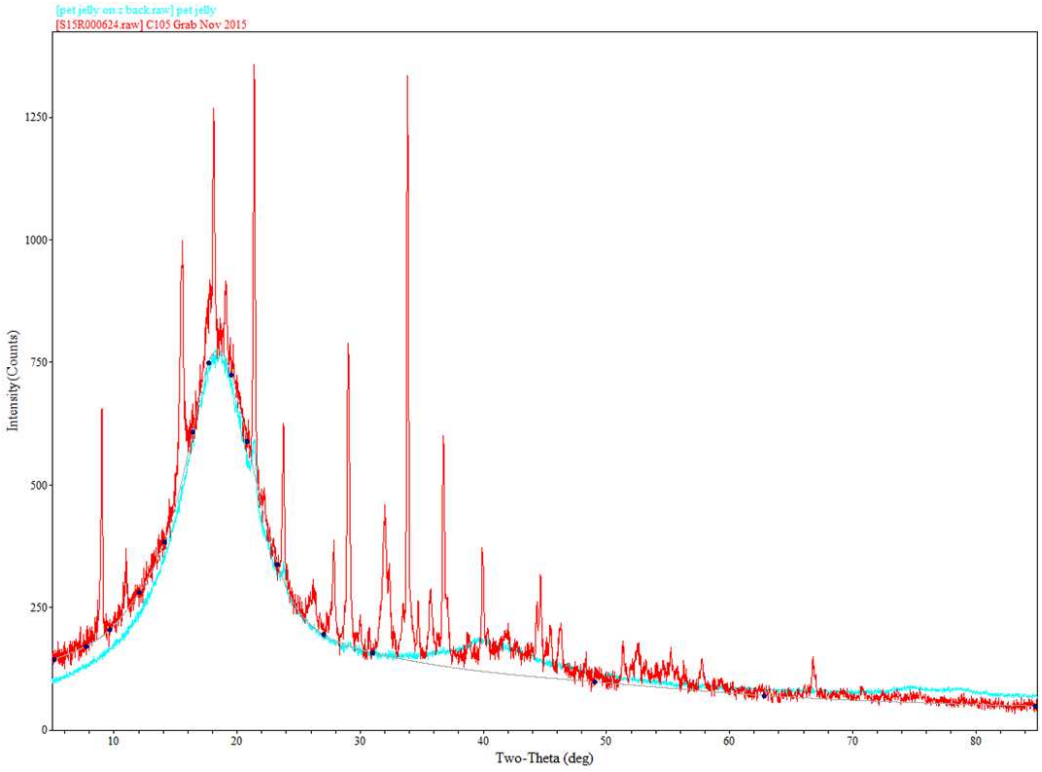

Figure 3. A Reference Pattern for Petroleum Jelly (Light Blue) Was Overlaid and Scaled to Match that of the Sample Data as an Estimate of the Shape of the Background Level.

Search Match: Each pattern was initially compared to the entire database with no other filters applied to the search process. Likely phases were selected from the returned results, and then

[2] Rigaku is a trademark of Rigaku/USA, Inc. The Woodlands, Texas.

additional increasingly more restrictive searches were performed. Typically, the second search was limited to the minerals subfile of the database and included a chemistry filter that was defined based primarily but not exclusively on energy dispersive spectrometry (EDS) data acquired for all four samples (i.e., H, C, N, O, F, Na, Al, Si, P, S, K, Ca, Cr, Mn, Fe, U). In some cases additional searches were performed by including the "Severe Orientation" filter and/or by searching the inorganic subfile of the database.

2.3 X-RAY DIFFRACTION RESULTS

Trona was identified in all of the samples as indicated in Table 2 below. Other major phases identified included cejkaite and dawsonite.

Table 2. X-ray Diffraction Phase Content Summary by Sample.

Phase Name	Formula	S15R622	S15R623	S15R624	S15R625
Trona	Na3H(CO3)2(H2O)2	M	m	M	M
Cejkaite	Na4(UO2)(CO3)3	M	M	------	------
Dawsonite	NaAlCO3(OH)2	------	M	M	M
Gibbsite	Al(OH)3	------	m	------	------
Natrophosphate	Na7F(PO4)2*19H2O	------	------	t	------
Unidentified peaks		2	1	6	1

M- major
m- minor
t- trace

Individual sample analysis results are presented in the following sections.

2.3.1 C-105 Grab Sample – S15R000622

The diffraction data for this sample indicates that it was principally comprised of trona and cejkaite as indicated in Figure 4 and Table 3. Two weak diffraction peaks remained unidentified. These peaks did not match any of the phases listed in Table 2. The peaks may be due to a trace phase that is statistically oriented.

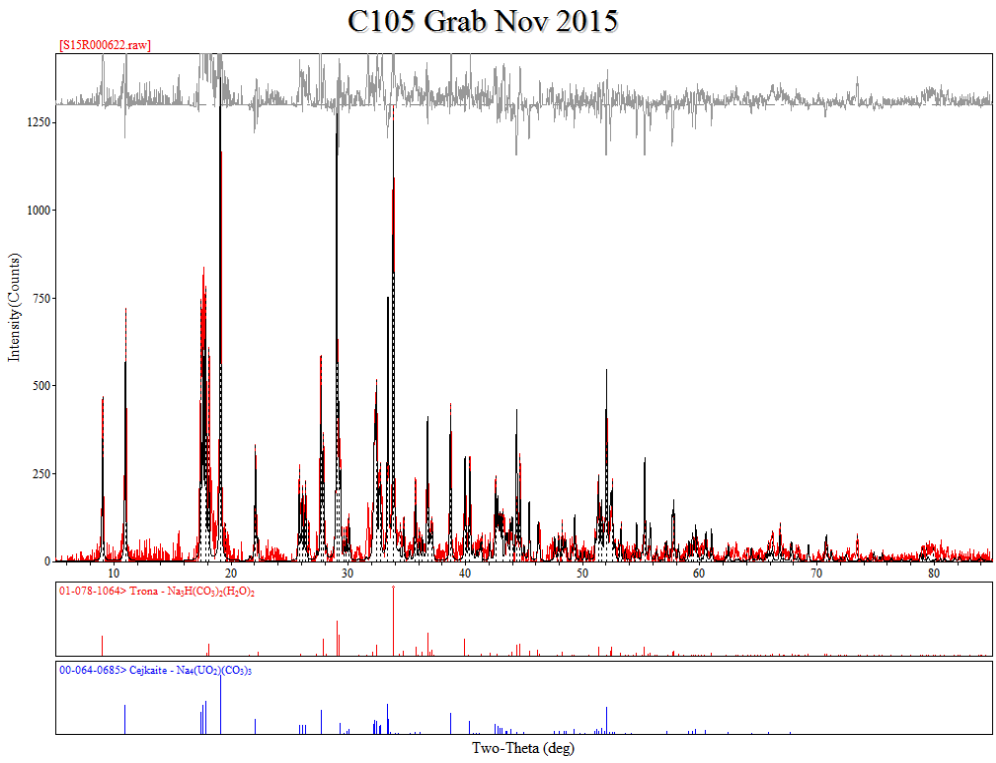

Figure 4. Phase Content for S15R000622.

Table 3. Diffraction Peak Data and Phase Association for S15R000622.

Peak ID Extended Report (74 Peaks, Max P/N = 18.4)
[S15R000622.raw] C105 Grab Nov 2015 - C105 Grab Nov 2015
PEAK: 17(pts)/Parabolic Filter, Threshold=3.0, Cutoff=1.1%, BG=3/1.0, Peak-Top=Summit

2-Theta	d(Å)	Height	Height%	Phase ID	d(Å)	I%	(h k l)	2-Theta	Delta
9.074	9.7376	460	33.7	Trona	9.7928	27.7	(2 0 0)	9.023	-0.051
11.034	8.0123	706	51.7	Cejkaite	8.058	42	(0 2 0)	10.971	-0.063
17.459	5.0753	722	52.9	Cejkaite	5.084	31	(-1 1 1)	17.429	-0.030
17.82	4.9735	762	55.8	Cejkaite	4.971	47	(1 1 1)	17.829	0.009
18.104	4.8959	588	43	Trona	4.8964	17	(4 0 0)	18.103	-0.002
19.101	4.6425	1367	100	Cejkaite	4.647	100	(1 3 0)	19.083	-0.018
19.485	4.5519	100	7.3	Unknown					
22.08	4.0225	316	23.1	Cejkaite	4.025	22	(0 4 0)	22.066	-0.014
25.838	3.4453	267	19.6	Cejkaite	3.45	13	(-2 2 1)	25.803	-0.036
26.101	3.4113	208	15.2	Cejkaite	3.415	13	(0 4 1)	26.072	-0.029
26.343	3.3805	222	16.2	Cejkaite	3.38	13	(2 2 1)	26.347	0.004
26.641	3.3433	104	7.6	Unknown					
27.659	3.2226	573	41.9	Cejkaite	3.22	35	(0 0 2)	27.681	0.022
27.881	3.1974	355	26	Trona	3.1985	23.6	(1 1 1)	27.871	-0.009
29.04	3.0723	734	53.7	Trona	3.0745	49.6	(3 1 0)	29.019	-0.021
29.235	3.0523	353	25.9	Trona	3.0581	29.3	(-3 1 1)	29.178	-0.057
29.621	3.0134	80	5.9	Cejkaite	3.009	2	(-1 1 2)	29.665	0.044
29.843	2.9915	84	6.1	Cejkaite	2.9908	4	(0 2 2)	29.85	0.007
30.035	2.9728	118	8.6	Cejkaite	2.9687	7	(1 1 2)	30.077	0.042
32.418	2.7595	506	37	Trona	2.7606	15	(1 1 2)	32.405	-0.013
32.739	2.7332	269	19.7	Cejkaite	2.7326	13	(2 4 1)	32.746	0.007
33.38	2.6822	702	51.4	Cejkaite	2.6839	43	(0 6 0)	33.358	-0.022
33.842	2.6466	1285	94	Trona	2.6463	100	(-5 1 1)	33.846	0.004
34.423	2.6032	88	6.4	Trona	2.6063	1.9	(5 1 0)	34.381	-0.042
34.74	2.5802	107	7.8	Trona	2.5819	7	(-2 0 4)	34.717	-0.023
35.723	2.5114	216	15.8	Trona	2.5097	11.7	(-5 1 2)	35.748	0.025
36.054	2.4891	77	5.6	Cejkaite	2.4873	3	(2 2 2)	36.081	0.027
36.267	2.475	48	3.5	Trona	2.4712	4.5	(3 1 2)	36.324	0.057
36.758	2.4431	353	25.8	Trona	2.4431	32.5	(-1 1 3)	36.757	0.000
37.099	2.4213	111	8.2	Trona	2.4191	7.5	(-3 1 3)	37.136	0.036
38.738	2.3226	419	30.6	Cejkaite	2.3241	30	(2 6 0)	38.712	-0.026
39.977	2.2534	253	18.5	Trona	2.2547	23.6	(2 0 4)	39.954	-0.023
40.366	2.2326	271	19.8	Cejkaite	2.2327	19	(1 7 0)	40.364	-0.002
41.395	2.1795	52	3.8	Trona	2.184	2	(-7 1 2)	41.305	-0.090
42.581	2.1215	215	15.7	Cejkaite	2.1224	14	(-4 2 1)	42.561	-0.019
43.158	2.0944	124	9	Cejkaite	2.0978	9	(3 5 1)	43.085	-0.073
43.762	2.0669	94	6.9	Trona	2.0698	1	(-3 1 4)	43.697	-0.065

2-Theta	d(Å)	Height	Height%	Phase ID	d(Å)	I%	(h k l)	2-Theta	Delta
44.015	2.0556	67	4.9	Trona	2.0568	4.5	(-1 1 4)	43.988	-0.026
44.363	2.0403	174	12.7	Trona	2.0406	15.6	(7 1 1)	44.355	-0.008
44.658	2.0275	288	21.1	Trona	2.0284	17.3	(-10,0,2)	44.637	-0.020
47.937	1.8962	65	4.7	Cejkaite	1.8952	4	(-2 6 2)	47.963	0.026
48.243	1.8849	93	6.8	Trona	1.8851	5.4	(-9 1 2)	48.236	-0.007
49.324	1.8461	108	7.9	Trona	1.8468	1.6	(9 1 0)	49.303	-0.021
51.358	1.7776	223	16.3	Cejkaite	1.7776	5	(-3 1 3)	51.359	0.000
51.638	1.7686	132	9.7	Cejkaite	1.7689	4	(3 7 1)	51.63	-0.008
52.056	1.7554	423	31	Trona	1.7551	0.7	(-1 1 5)	52.066	0.011
52.516	1.7411	207	15.1	Trona	1.7417	12.7	(9 1 1)	52.497	-0.019
53.049	1.7249	39	2.8	Trona	1.7194	3.7	(-4 0 6)	53.232	0.183
53.279	1.718	97	7.1	Trona	1.7194	3.7	(2 2 0)	53.232	-0.047
54.516	1.6819	42	3	Trona	1.6793	4.3	(2 2 1)	54.607	0.091
55.298	1.6599	115	8.4	Trona	1.6604	11.8	(-7 1 5)	55.28	-0.018
57.053	1.613	47	3.4	Cejkaite	1.6106	4	(0,10,0)	57.144	0.091
57.783	1.5943	121	8.9	Trona	1.5944	6.5	(-11,1,3)	57.778	-0.005
58.823	1.5686	40	2.9	Trona	1.5736	0.9	(3 1 5)	58.619	-0.204
59.025	1.5637	39	2.9	Cejkaite	1.5627	4	(0,10,1)	59.066	0.041
59.274	1.5577	51	3.7	Trona	1.5566	1.5	(-2 2 3)	59.322	0.048
59.464	1.5532	60	4.4	Trona	1.5529	1	(-6 2 1)	59.476	0.013
59.813	1.545	61	4.5	Trona	1.5438	0.5	(-3 1 6)	59.862	0.049
60.159	1.5369	43	3.1	Trona	1.5373	0.2	(6 2 0)	60.144	-0.015
60.519	1.5286	60	4.4	Cejkaite	1.5289	6	(4 2 3)	60.507	-0.013
60.983	1.5181	23	1.7	Trona	1.518	3.7	(4 2 2)	60.986	0.003
62.386	1.4873	37	2.7	Trona	1.4871	0.1	(-10,0,6)	62.394	0.007
64.039	1.4528	27	1.9	Trona	1.4513	0.2	(5 1 5)	64.113	0.074
65.876	1.4167	41	3	Cejkaite	1.4172	3	(-6 4 1)	65.849	-0.027
66.162	1.4113	71	5.2	Trona	1.4108	1.7	(-9 1 6)	66.185	0.023
66.855	1.3983	83	6.1	Trona	1.399	3	(-14,0,4)	66.818	-0.037
67.106	1.3937	38	2.8	Trona	1.3936	0.5	(-6 2 4)	67.11	0.004
67.84	1.3804	44	3.2	Trona	1.3803	1.7	(3 1 6)	67.844	0.003
68.355	1.3712	31	2.3	Trona	1.3712	1.2	(-12,0,6)	68.357	0.002
70.801	1.3297	59	4.3	Trona	1.3298	2.8	(6 0 6)	70.798	-0.004
73.45	1.2882	66	4.8	Trona	1.2867	0.4	(1 1 7)	73.551	0.101
78.964	1.2115	34	2.5	Trona	1.2107	0.7	(4 2 5)	79.023	0.059
79.338	1.2067	40	2.9	Trona	1.2063	0.3	(-3 1 8)	79.368	0.030
79.935	1.1992	26	1.9	Trona	1.1997	0.3	(0 2 6)	79.891	-0.044

Ave. = -0.002
St. Dev. = 0.050

2.3.2 C-105 Grab Sample – S15R000623

The diffraction data for this sample indicates that it was principally comprised of cejkaite, dawsonite, trona, and gibbsite as indicated in Figure 5 and Table 4. One weak diffraction peak remained unidentified. This peak did not match any of the phases listed in Table 2. The peak may be due to a trace phase that is statistically oriented.

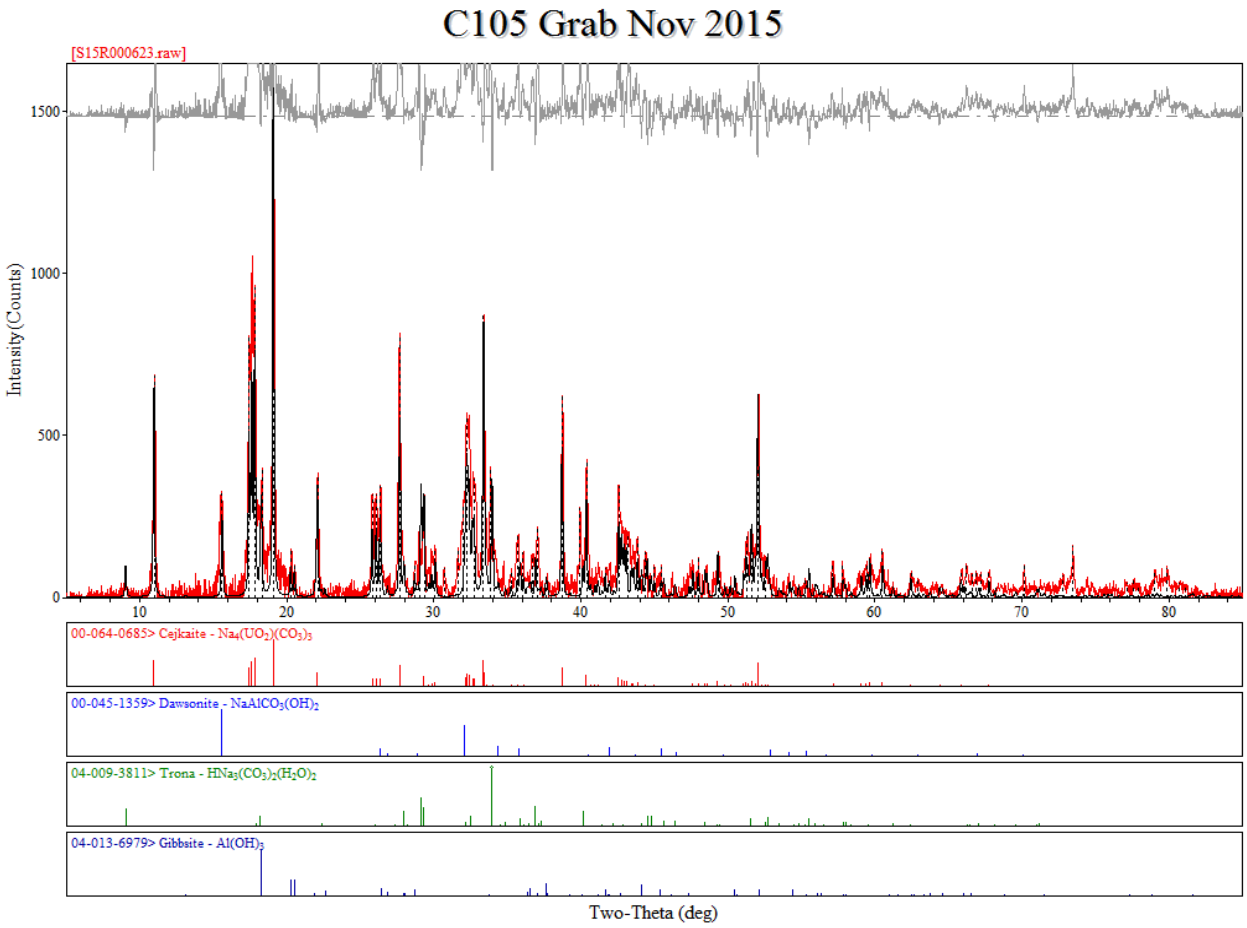

Figure 5. Phase Content for S15R000623.

Table 4. Diffraction Peak Data and Phase Association for S15R000623.

Peak ID Extended Report (73 Peaks, Max P/N = 18.7)
[S15R000623.raw] C105 Grab Nov 2015 - C105 Grab Nov 2015
PEAK: 21(pts)/Parabolic Filter, Threshold=3.0, Cutoff=1.1%, BG=3/1.0, Peak-Top=Summit

2-Theta	d(Å)	Height	Height%	Phase ID	d(Å)	I%	(h k l)	2-Theta	Delta
11.02	8.0221	684	46.2	Cejkaite	8.058	42	(0 2 0)	10.971	-0.049
15.54	5.6974	311	21	Dawsonite	5.6744	100	(0 1 1)	15.604	0.063
17.459	5.0754	768	51.8	Cejkaite	5.084	31	(-1 1 1)	17.429	-0.030
17.82	4.9733	929	62.8	Cejkaite	4.971	47	(1 1 1)	17.829	0.008
18.337	4.8344	368	24.9	Gibbsite	4.8509	100	(0 0 2)	18.274	-0.063
19.102	4.6424	1481	100	Cejkaite	4.647	100	(1 3 0)	19.083	-0.019
20.321	4.3665	141	9.5	Gibbsite	4.3779	26.7	(1 1 0)	20.268	-0.053
20.53	4.3227	92	6.2	Gibbsite	4.326	26	(2 0 0)	20.514	-0.016
22.1	4.019	370	25	Cejkaite	4.025	22	(0 4 0)	22.066	-0.033
25.82	3.4477	304	20.6	Cejkaite	3.45	13	(-2 2 1)	25.803	-0.017
26.062	3.4162	306	20.7	Cejkaite	3.415	13	(0 4 1)	26.072	0.010
26.379	3.376	319	21.6	Cejkaite	3.38	13	(2 2 1)	26.347	-0.032
27.661	3.2223	804	54.3	Cejkaite	3.22	35	(0 0 2)	27.681	0.020
28.741	3.1036	93	6.3	Gibbsite	3.1077	9.9	(-1 0 3)	28.702	-0.039
29.02	3.0744	188	12.7	Trona	3.0625	47	(3 1 0)	29.135	0.115
29.361	3.0395	302	20.4	Cejkaite	3.042	16	(2 4 0)	29.336	-0.024
30.061	2.9703	148	10	Cejkaite	2.9687	7	(1 1 2)	30.077	0.016
30.702	2.9097	80	5.4	Unknown					
31.638	2.8258	131	8.9	Trona	2.8251	0.5	(3 1 1)	31.645	0.007
32.002	2.7944	266	17.9	Dawsonite	2.7875	50	(1 2 1)	32.084	0.082
32.26	2.7727	548	37	Cejkaite	2.7714	20	(-2 4 1)	32.275	0.015
32.779	2.7299	349	23.6	Gibbsite	2.7274	0.1	(0 1 3)	32.811	0.031
33.381	2.682	852	57.5	Cejkaite	2.6839	43	(0 6 0)	33.358	-0.024
33.861	2.6452	376	25.4	Trona	2.6379	100	(-5 1 1)	33.956	0.096
34.097	2.6274	135	9.1	Cejkaite	2.6314	2	(1 3 2)	34.043	-0.054
35.276	2.5422	64	4.3	Cejkaite	2.5441	2	(-2 2 2)	35.249	-0.027
35.735	2.5106	171	11.6	Gibbsite	2.5075	0.1	(3 1 0)	35.781	0.046
36.078	2.4875	110	7.4	Cejkaite	2.4873	3	(2 2 2)	36.081	0.003
36.742	2.4441	109	7.4	Gibbsite	2.4352	0.8	(1 2 0)	36.881	0.139
37.041	2.425	202	13.6	Gibbsite	2.4255	3.5	(0 0 4)	37.034	-0.007
37.661	2.3865	47	3.1	Gibbsite	2.3879	19.8	(3 1 1)	37.639	-0.023
38.741	2.3225	601	40.6	Cejkaite	2.3241	30	(2 6 0)	38.712	-0.028
39.942	2.2553	245	16.5	Gibbsite	2.2487	3.2	(0 2 2)	40.066	0.123
40.382	2.2317	385	26	Cejkaite	2.2327	19	(1 7 0)	40.364	-0.018
41.718	2.1633	46	3.1	Gibbsite	2.167	10.4	(4 0 0)	41.645	-0.074
42.598	2.1206	296	20	Cejkaite	2.1224	14	(-4 2 1)	42.561	-0.037
43.241	2.0906	150	10.1	Gibbsite	2.0862	0.3	(1 1 4)	43.337	0.097

Ave. = 0.0088
St. Dev. 0.0577

2-Theta	d(Å)	Height	Height%	Phase ID	d(Å)	I%	(h k l)	2-Theta	Delta
43.857	2.0627	157	10.6	Cejkaite	2.0631	7	(1 1 3)	43.847	-0.010
44.384	2.0394	99	6.7	Cejkaite	2.0394	3	(3 3 2)	44.383	0.000
45.009	2.0125	84	5.7	Gibbsite	2.012	0.4	(-2 1 4)	45.02	0.011
45.442	1.9943	84	5.7	Dawsonite	1.9926	12	(0 1 5)	45.484	0.042
47.567	1.9101	72	4.9	Cejkaite	1.9088	5	(4 4 1)	47.601	0.034
47.983	1.8945	112	7.5	Trona	1.8937	1	(-9 1 1)	48.003	0.019
49.344	1.8453	124	8.4	Cejkaite	1.8469	8	(2 8 0)	49.3	-0.044
51.318	1.7789	187	12.6	Gibbsite	1.7797	1.2	(2 2 3)	51.295	-0.023
51.6	1.7698	201	13.6	Cejkaite	1.7703	9	(2 8 1)	51.586	-0.014
52.075	1.7548	612	41.3	Gibbsite	1.7534	10	(0 2 4)	52.119	0.044
52.541	1.7404	102	6.9	Cejkaite	1.7401	3	(2 4 3)	52.549	0.009
55.239	1.6616	50	3.4	Trona	1.6613	1.4	(10,0,2)	55.249	0.010
57.117	1.6113	98	6.6	Cejkaite	1.6106	4	(0,10,0)	57.144	0.028
57.781	1.5944	98	6.6	Gibbsite	1.5933	2.4	(5 1 1)	57.823	0.042
59.439	1.5538	99	6.7	Gibbsite	1.5539	0.3	(4 0 4)	59.436	-0.003
59.661	1.5485	121	8.2	Gibbsite	1.5482	0.4	(2 3 1)	59.676	0.015
60.482	1.5295	132	8.9	Cejkaite	1.5289	6	(4 2 3)	60.507	0.024
62.457	1.4858	62	4.2	Gibbsite	1.4855	1.5	(-1 3 3)	62.471	0.014
62.904	1.4763	51	3.5	Gibbsite	1.4765	0.3	(5 0 3)	62.896	-0.009
65.899	1.4162	77	5.2	Trona	1.4172	0.9	(8 2 0)	65.852	-0.047
66.22	1.4102	93	6.3	Trona	1.4093	1.5	(-13,1,3)	66.268	0.048
66.597	1.4031	57	3.9	Gibbsite	1.404	3.3	(-3 1 6)	66.546	-0.052
66.877	1.3979	63	4.3	Dawsonite	1.3959	4	(4 0 0)	66.983	0.106
67.178	1.3924	60	4	Dawsonite	1.3939	1	(2 4 2)	67.092	-0.086
67.742	1.3821	68	4.6	Gibbsite	1.3821	0.3	(3 3 2)	67.743	0.001
68.26	1.3729	18	1.2	Trona	1.371	0.4	(8 2 1)	68.369	0.109
70.119	1.341	85	5.8	Gibbsite	1.3407	0.1	(-5 2 3)	70.135	0.015
72.74	1.299	49	3.3	Trona	1.2984	0.7	(-6 2 5)	72.777	0.037
73.438	1.2884	142	9.6	Dawsonite	1.2896	1	(2 1 7)	73.356	-0.082
77.122	1.2357	33	2.3	Trona	1.2334	0.1	(0 0 8)	77.295	0.173
77.6	1.2293	45	3	Gibbsite	1.2287	0.3	(0 4 2)	77.648	0.048
77.902	1.2253	32	2.2	Trona	1.2254	0.1	(-13,1,6)	77.896	-0.006
79.024	1.2107	65	4.4	Dawsonite	1.2094	1	(2 5 1)	79.129	0.104
79.823	1.2006	62	4.2	Trona	1.2004	0.6	(-3 1 8)	79.834	0.011
80.683	1.1899	41	2.7	Gibbsite	1.1895	0.4	(-5 3 2)	80.721	0.038
81.074	1.1852	33	2.2	Gibbsite	1.1873	0.2	(-7 0 3)	80.9	-0.174

2.3.3 C-105 Grab Sample – S15R000624

The diffraction data for this sample indicates that it was principally comprised of trona, dawsonite, and natrophosphate as indicated in Figure 6 and Table 5. Six relatively weak diffraction peaks remained unidentified. These peaks did not match any of the phases listed in Table 2. These peaks may have been more difficult to identify because this data set was noisier than the others (i.e., the data acquisition rate was 2x faster than the other three data sets). It is also possible that one or more trace phases were statistically oriented yielding insufficient diffraction data for the associated phases to be identified.

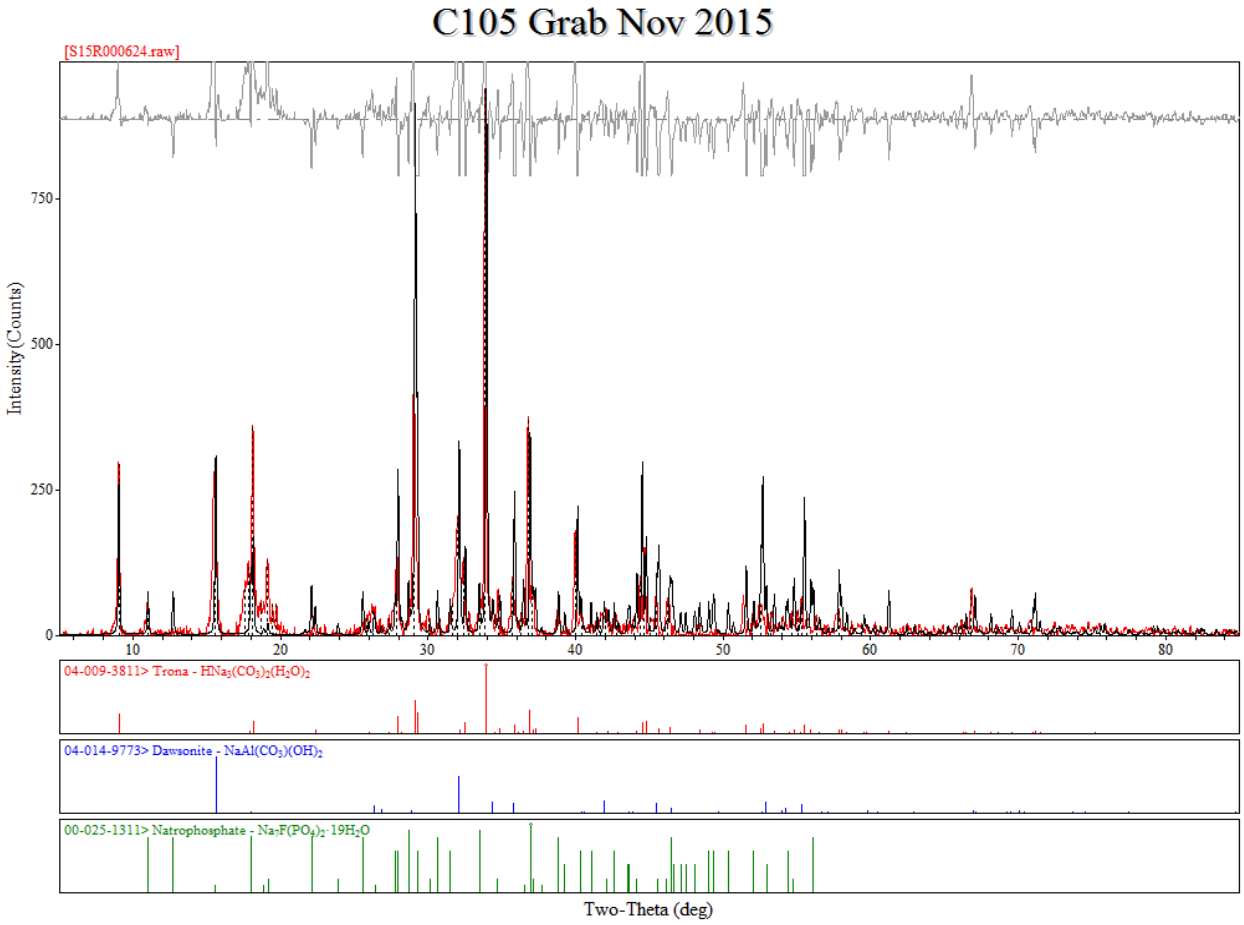

Figure 6. Phase Content for S15R000624.

Table 5. Diffraction Peak Data and Phase Association for S15R000624.

Peak ID Extended Report (66 Peaks, Max P/N = 15.1)
[S15R000624.raw] C105 Grab Nov 2015 - C105 Garb Nov 2015
PEAK: 21(pts)/Parabolic Filter, Threshold=3.0, Cutoff=1.1%, BG=3/1.0, Peak-Top=Summit

2-Theta	d(Å)	Height	Height%	Phase ID	d(Å)	I%	(h k l)	2-Theta	Delta
9.04	9.7747	295	31.8	Trona	9.7618	27.7	(2 0 0)	9.052	0.012
11.018	8.0238	65	7	Natrophosphate	8.02	80	(2 2 2)	11.023	0.005
15.56	5.6902	289	31.2	Natrophosphate	5.68	10	(4 2 2)	15.588	0.028
17.602	5.0346	67	7.2	Trona	5.0128	0.2	(-2 0 2)	17.679	0.077
17.82	4.9735	104	11.2	Unknown					
18.12	4.8918	348	37.5	Trona	4.8809	16.9	(4 0 0)	18.161	0.041
18.661	4.7511	47	5.1	Natrophosphate	4.7	10	(5 3 1)	18.866	0.205
19.138	4.6337	123	13.3	Natrophosphate	4.63	20	(4 4 2)	19.154	0.015
19.459	4.558	47	5.1	Unknown					
19.72	4.4984	46	5	Unknown					
22.222	3.9972	31	3.3	Natrophosphate	4.02	90	(4 4 4)	22.094	-0.128
25.842	3.4448	29	3.1	Trona	3.426	2.2	(1 1 0)	25.987	0.145
26.237	3.3938	44	4.7	Dawsonite	3.3795	11.1	(2 0 0)	26.351	0.113
27.359	3.2572	28	3	Trona	3.2539	1.8	(6 0 0)	27.387	0.028
27.881	3.1974	131	14.2	Natrophosphate	3.19	60	(6 6 2)	27.947	0.066
29.04	3.0723	447	48.3	Trona	3.0625	47	(4 0 2)	29.135	0.095
30.021	2.9742	37	4	Natrophosphate	2.964	20	(6 6 4)	30.126	0.106
30.802	2.9005	24	2.6	Natrophosphate	2.915	80	(9 3 1)	30.645	-0.157
31.645	2.8252	37	4	Trona	2.8251	0.5	(3 1 1)	31.645	0.000
32	2.7946	200	21.5	Dawsonite	2.7862	53.2	(2 1 1)	32.099	0.099
32.399	2.7611	126	13.6	Trona	2.7506	15.6	(1 1 2)	32.526	0.127
32.775	2.7302	33	3.6	Unknown					
33.48	2.6743	54	5.8	Natrophosphate	2.675	90	(10,2,2)	33.472	-0.009
33.86	2.6452	927	100	Trona	2.6379	100	(-5 1 1)	33.956	0.097
34.739	2.5803	68	7.4	Natrophosphate	2.582	20	(8 6 4)	34.715	-0.024
35.72	2.5116	90	9.7	Dawsonite	2.5053	13.9	(1 2 1)	35.814	0.094
36.296	2.473	30	3.3	Trona	2.4623	4.4	(0 0 4)	36.461	0.164
36.762	2.4428	365	39.3	Trona	2.434	33.4	(-1 1 3)	36.9	0.138
37.038	2.4252	76	8.2	Natrophosphate	2.429	100	(10,4,4)	36.978	-0.060
39.96	2.2544	170	18.3	Trona	2.2451	23.7	(2 0 4)	40.131	0.172
40.379	2.2319	33	3.6	Natrophosphate	2.233	60	(11,5,3)	40.359	-0.020
41.441	2.1771	19	2	Trona	2.1771	1.9	(-7 1 2)	41.442	0.000
41.682	2.1651	29	3.1	Unknown					

Ave. = 0.056
St.Dev. = 0.091

2-Theta	d(Å)	Height	Height%	Phase ID	d(Å)	I%	(h k l)	2-Theta	Delta
42.04	2.1475	39	4.2	Natrophosphate	2.145	20	(10,8,2)	42.091	0.051
42.749	2.1135	21	2.2	Trona	2.1076	2.1	(3 1 3)	42.875	0.126
43.943	2.0588	26	2.8	Trona	2.0621	1	(-3 1 4)	43.87	-0.073
44.361	2.0404	93	10	Trona	2.034	15.8	(-7 1 3)	44.508	0.146
44.661	2.0274	144	15.5	Trona	2.0222	17.1	(-10,0,2)	44.78	0.119
45.08	2.0095	24	2.6	Unknown					
45.46	1.9936	65	7	Dawsonite	1.9924	13.7	(2 2 2)	45.489	0.029
46.218	1.9626	61	6.6	Natrophosphate	1.966	20	(14,2,0)	46.134	-0.084
48.341	1.8813	22	2.3	Trona	1.8793	5.6	(-9 1 2)	48.395	0.054
51.962	1.7584	33	3.6	Natrophosphate	1.755	60	(15,5,1)	52.069	0.107
52.52	1.741	43	4.7	Trona	1.74	6.7	(6 0 4)	52.552	0.032
53.021	1.7257	29	3.1	Natrophosphate	1.728	40	(12,10,4)	52.946	-0.075
53.263	1.7184	32	3.4	Trona	1.7124	3.7	(2 2 0)	53.467	0.204
54.023	1.696	20	2.2	Dawsonite	1.697	3.2	(1 3 2)	53.989	-0.034
54.638	1.6784	27	2.9	Natrophosphate	1.676	20	(16,4,2)	54.723	0.085
55.04	1.6671	33	3.6	Trona	1.6613	1.4	(10,0,2)	55.249	0.208
55.298	1.6599	57	6.1	Dawsonite	1.6597	12.3	(2 2 4)	55.305	0.007
55.7	1.6489	19	2	Trona	1.6543	12.5	(7 1 3)	55.503	-0.197
56.319	1.6322	29	3.2	Dawsonite	1.6302	0.4	(3 1 4)	56.395	0.077
57.838	1.5929	38	4	Trona	1.5925	5.8	(4 2 1)	57.856	0.018
58.698	1.5716	19	2.1	Trona	1.5672	0.9	(3 1 5)	58.879	0.180
59.342	1.5561	14	1.5	Trona	1.5513	1.7	(-2 2 3)	59.545	0.204
60.282	1.5341	17	1.8	Trona	1.5344	0.2	(6 2 0)	60.267	-0.015
62.461	1.4857	18	1.9	Trona	1.4863	1.3	(6 2 1)	62.432	-0.029
66.14	1.4117	21	2.3	Trona	1.4093	1.5	(-13,1,3)	66.268	0.128
66.423	1.4063	14	1.6	Trona	1.406	1.9	(-9 1 6)	66.444	0.021
66.819	1.399	77	8.3	Dawsonite	1.3963	3.6	(0 4 0)	66.966	0.146
68.5	1.3687	14	1.5	Trona	1.3666	1.2	(-12,0,6)	68.621	0.122
69.179	1.3569	12	1.3	Dawsonite	1.3558	1.4	(1 4 1)	69.244	0.065
70.78	1.3301	21	2.3	Trona	1.3267	2.3	(-2 2 5)	70.984	0.204
72.441	1.3036	18	2	Dawsonite	1.3031	0.7	(0 0 8)	72.472	0.031
74.722	1.2694	17	1.9	Trona	1.2693	0.1	(-2 0 8)	74.728	0.006
75.518	1.258	14	1.5	Dawsonite	1.2571	1	(3 3 4)	75.576	0.058

2.3.4 C-105 Grab Sample – S15R000625

The diffraction data for this sample indicates that the tan aggregate was principally comprised of trona and dawsonite, as indicated in Figure 7 and Table 6. One weak diffraction peak remained unidentified. This peak did not match any of the phases listed in Table 2. The peak may be due to a trace phase that is statistically oriented.

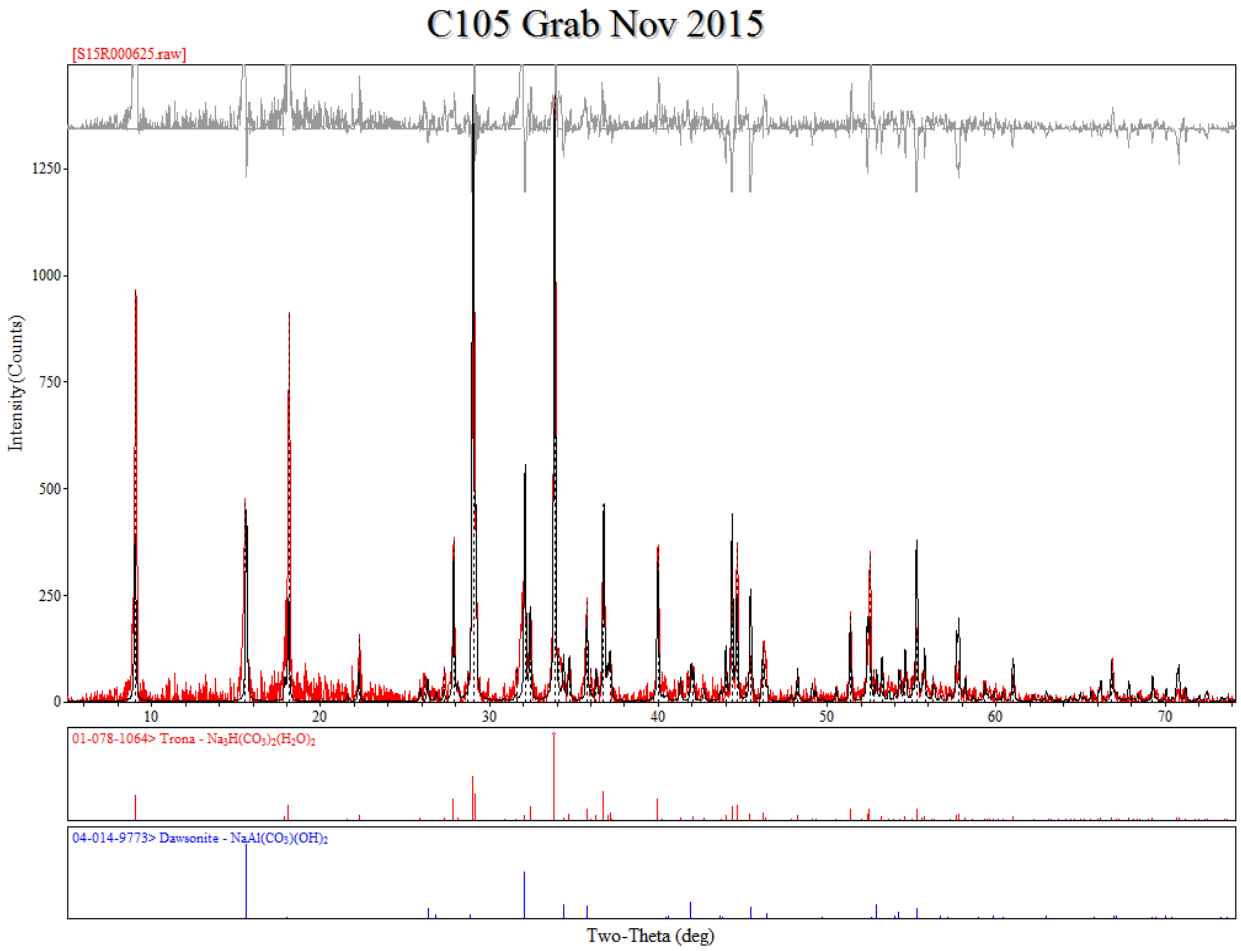

Figure 7. Phase Content for S15R000625.

Table 6. Diffraction Peak Data and Phase Association for S15R000625.

Peak ID Extended Report (44 Peaks, Max P/N = 18.7)
[S15R000625.raw] C105 Grab Nov 2015 - C105 Grab Nov 2015
PEAK: 15(pts)/Parabolic Filter, Threshold=3.0, Cutoff=1.1%, BG=3/1.0, Peak-Top=Summit

2-Theta	d(Å)	Height	Height%	Phase ID	d(Å)	I%	(h k l)	2-Theta	Delta
9.063	9.7501	956	67.9	Trona	9.7928	27.7	(2 0 0)	9.023	-0.04
15.523	5.7038	464	32.9	Dawsonite	5.6713	100	(1 0 1)	15.612	0.089
18.155	4.8823	879	62.4	Trona	4.8964	17	(4 0 0)	18.103	-0.053
22.313	3.981	149	10.6	Trona	3.9893	4.7	(2 0 2)	22.266	-0.047
26.175	3.4018	50	3.6	Dawsonite	3.3795	11.1	(2 0 0)	26.351	0.176
27.355	3.2576	70	5	Trona	3.2643	1.7	(6 0 0)	27.298	-0.057
27.879	3.1976	368	26.2	Trona	3.1985	23.6	(1 1 1)	27.871	-0.008
28.738	3.104	54	3.8	Dawsonite	3.0905	4.5	(1 0 3)	28.866	0.128
29.06	3.0703	1186	84.3	Trona	3.0745	49.6	(4 0 2)	29.019	-0.04
31.598	2.8292	73	5.2	Trona	2.8348	0.5	(3 1 1)	31.534	-0.064
32.119	2.7846	241	17.1	Dawsonite	2.7862	53.2	(0 2 0)	32.099	-0.019
32.404	2.7607	205	14.5	Trona	2.7606	15	(1 1 2)	32.405	0.001
33.86	2.6452	1408	100	Trona	2.6463	100	(-5 1 1)	33.846	-0.014
34.081	2.6286	119	8.4	Unknown					
34.756	2.579	94	6.7	Trona	2.5819	7	(-2 0 4)	34.717	-0.04
35.759	2.509	205	14.5	Trona	2.5097	11.7	(-5 1 2)	35.748	-0.011
35.999	2.4928	71	5	Trona	2.4932	1.2	(-8 0 2)	35.994	-0.006
36.284	2.4739	68	4.8	Trona	2.4712	4.5	(3 1 2)	36.324	0.04
36.76	2.4429	447	31.8	Trona	2.4431	32.5	(-1 1 3)	36.757	-0.003
37.156	2.4178	108	7.7	Trona	2.4191	7.5	(-3 1 3)	37.136	-0.021
39.978	2.2534	349	24.8	Trona	2.2547	23.6	(2 0 4)	39.954	-0.024
41.741	2.1622	54	3.8	Dawsonite	2.1527	18.2	(2 2 0)	41.934	0.193

2-Theta	d(Å)	Height	Height%	Phase ID	d(Å)	I%	(h k l)	2-Theta	Delta
42.039	2.1476	71	5	Trona	2.1461	4.3	(5 1 2)	42.07	0.031
44.038	2.0546	64	4.5	Trona	2.0568	4.5	(-1 1 4)	43.988	-0.049
44.378	2.0396	236	16.8	Trona	2.0406	15.6	(-7 1 3)	44.355	-0.023
44.659	2.0275	357	25.4	Trona	2.0284	17.3	(-10,0,2)	44.637	-0.022
45.16	2.0061	41	2.9	Trona	1.9947	6.8	(-5 1 4)	45.434	0.274
45.474	1.993	90	6.4	Dawsonit	1.9924	13.7	(2 2 2)	45.489	0.015
46.239	1.9618	127	9	Trona	1.964	8.6	(1 1 4)	46.184	-0.055
48.231	1.8853	42	3	Trona	1.8851	5.4	(-9 1 2)	48.236	0.005
51.378	1.777	196	13.9	Trona	1.7781	12.3	(-3 1 5)	51.345	-0.034
52.537	1.7405	336	23.8	Trona	1.7417	12.7	(9 1 1)	52.497	-0.04
52.76	1.7336	56	4	Dawsonit	1.7375	1.6	(0 0 6)	52.634	-0.126
53.277	1.718	52	3.7	Trona	1.7194	3.7	(-4 0 6)	53.232	-0.044
54.603	1.6794	48	3.4	Trona	1.6793	4.3	(2 2 1)	54.607	0.004
55.037	1.6672	35	2.5	Trona	1.6672	1.2	(10,0,2)	55.038	0.001
55.315	1.6595	145	10.3	Dawsonit	1.6597	12.3	(2 2 4)	55.305	-0.01
55.794	1.6463	67	4.8	Trona	1.6476	4.3	(0 2 2)	55.748	-0.047
56.265	1.6337	37	2.6	Trona	1.6352	0.8	(-11,1,2)	56.209	-0.056
57.761	1.5949	75	5.3	Trona	1.5944	6.5	(-8 0 6)	57.778	0.017
59.341	1.5561	35	2.5	Trona	1.5566	1.5	(2 0 6)	59.322	-0.019
61.012	1.5174	57	4	Trona	1.518	3.7	(-1 1 6)	60.986	-0.026
66.859	1.3982	95	6.8	Trona	1.399	3	(14,0,0)	66.818	-0.041
69.267	1.3554	33	2.4	Trona	1.3558	1.9	(-5 1 7)	69.245	-0.022

Ave. = -0.002
St.Dev. 0.073

3 POLARIZED LIGHT MICROSCOPY

3.1 SAMPLE PREPARATION

Analysis by PLM was performed on grab samples from C-105 to characterize the solids that remained in the tank. The analysis of all C-105 samples consisted in mounting triplicate slides and analyzing them using PLM. Each of the three slides was prepped differently; one was mounted in 1.550 refractive index oil, the second one was mounted in water, and the final one was placed in 1.680 refractive index oil. Oil does not dissolve the sample, thus it is the preferred mounting medium. Water was used to determine what particles dissolved and confirmed the identification of some of the particles. The slides were examined at multiple magnifications using procedure LT-519-107 on the Nikon EclipsePOL in Room 1GA at the 222-S Laboratory.

3.2 DATA PROCESSING

S15R000625 (sample of the tan aggregrate in 105C-15-03) contained two large brown chunks, but when particles were crushed on the microscope slide the sample appeared more white than brown. This sub-sample was selected from the third grab sample based on its relatively light tan appearance in the sample jar. The samples for the photos below were mounted on a glass slide with a coverslip overtop of the particles. Refractive index oil of 1.550 was used for the first slide mount to accurately perform the analysis and preserve the actual state of the solids collected.

The PLM images in Figures 8 and 9 illustrate the descriptions below. The major phase consisted of aggregates of fine-grained material with a brownish color. This phase is most likely $NaAl(CO_3)(OH)_2$ (dawsonite) based on SEM analysis that detected a significant amount of aluminum, and XRD analysis confirmed the presence of dawsonite. This component appeared to be around 50% of the mass of the sample observed (white circles in figures). The next most dominant phase (black circles) was $Na_2CO_3 \cdot H_2O$ (sodium carbonate) and/or $Na_3(HCO_3)CO_3$ (trona), followed by $Na_4(UO_2)(CO_3)_3$ (cejkaite, red circles), then possibly $Al(OH)_3$ (gibbsite, blue circles), and finally trace amounts of sodium fluoride phosphate (not pictured) and iron-bearing particulates (not pictured).

The black particles in Figures 8 and 9 were ubiquitous in all of the samples analyzed. The particles are very tiny (sub-micron), mainly opaque, and tend to form a coating on all of the larger particles. Due to their apparent lack of X-ray signature in both the electron microscope and XRD analyses, they are speculated to be organic, and are probably polymeric.

The uranium-rich phase was identified as cejkaite by its refractive indexes ($n_o = 1.531$, $n_e = 1.645$). Mounted in 1.550 refractive index oil (slide 1), the cejkaite rods (greenish-yellow with uncrossed polars) were nearly invisible in the vertical orientation (refractive index of the crystal close to 1.550) and showed high contrast in the horizontal position with a Becke line that indicated the refractive index of the crystal was significantly higher than 1.550. Thus, the estimated refractive indexes of the crystal are consistent with the literature values for cejkaite.

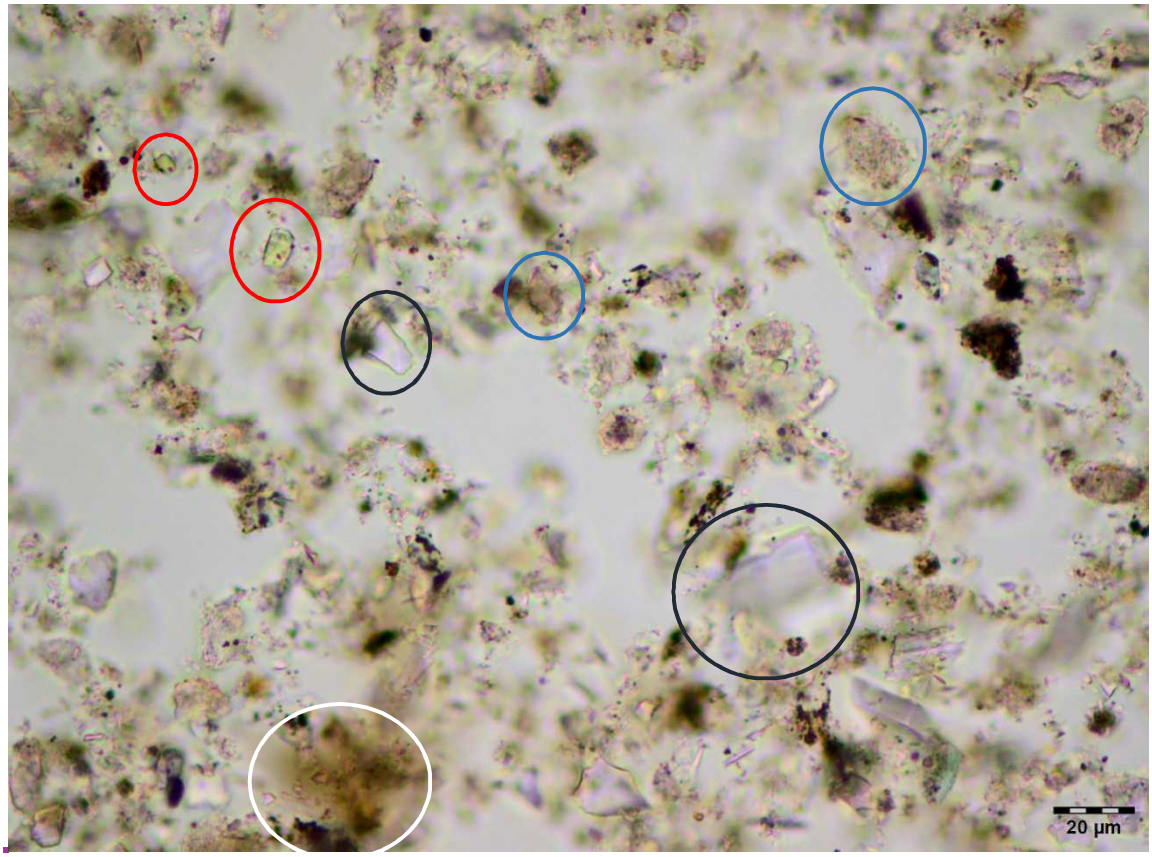

Figure 8. Sample S15R000625, Slide 1: Uncrossed Polars PLM Image of 3 Dominant Phases.

Uncrossed polars, highlighting the natural color and shape characteristics. White circle = dawsonite, Black = sodium carbonate and/or trona, Red = sodium uranium carbonate (cejkaite), Blue = gibbsite (tentative).

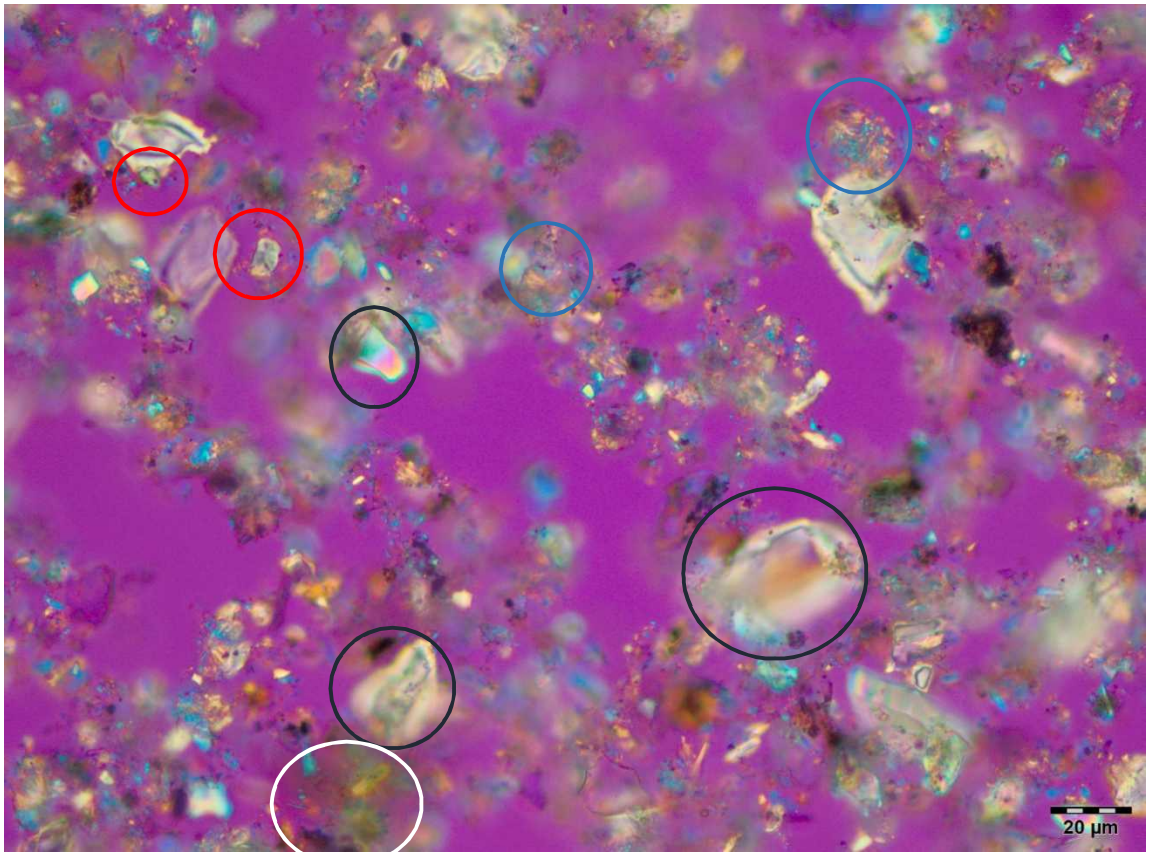

Figure 9. Sample S15R000625, Slide 1: Crossed Polars with Red I Compensator in Place.

Crossed polars with Red I compensator, emphasizing the optical properties of the particles; same field of view as Figure 8.

Slide 2 from sample S15R000625 was prepared in a fashion similar to the first slide except instead of using refractive index oil, the sample was prepared in water. Water will typically dissolve soluble salts such as nitrates, nitrites, and carbonates and leave behind minerals like gibbsite and iron oxide/hydroxide. In the second slide, the most prevalent phase is still dawsonite (Figure 10), but the second most dominant is the uranium phase. Sodium uranyl carbonate (cejkaite) is similar looking to sodium carbonate rods, but the orientation of the blue/orange crystal color when the Red I compensator is in place and the polars are crossed reveals that the colors are reversed for cejkaite. The orientation color at the 2 o'clock position is blue for cejkaite rods, and for carbonate rods it is orange in the 2 o'clock position. This color is demonstrated in Figure 11 and indicates that the cejkaite crystals are optically positive.

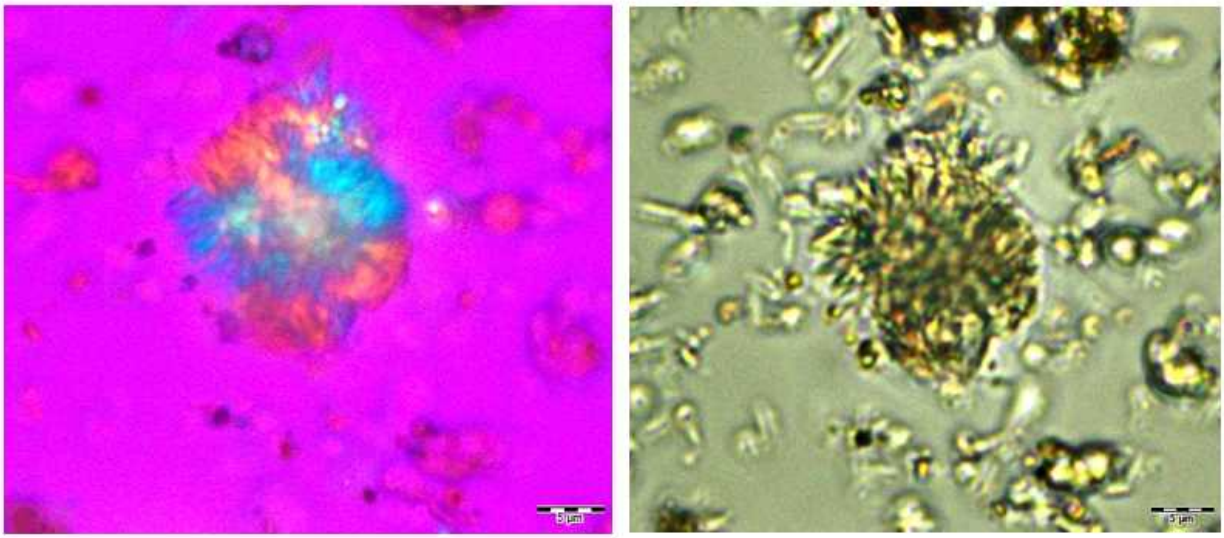

Figure 10. Sample S15R000625, Slide 2.

15-µm sized aggregate of dawsonite crystals; (left) photo has the Red 1 compensator in and polars crossed. The photo on the right is shown with uncrossed polars and no Red I compensator. Both images are of the same crystal.

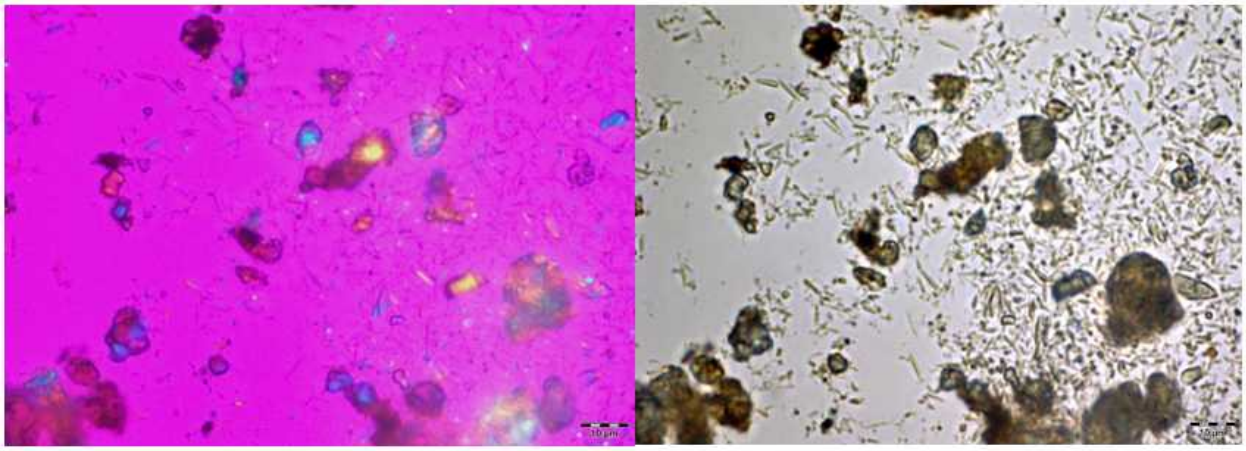

Figure 11. Sample S15R000625, Slide 2.

5-um long uranium crystals (needles). Photo on the left has the Red 1 compensator in and polars crossed. The photo on the right is shown with uncrossed polars and no Red I compensator. Both images are of the same area.

Slide 3 for sample S15R000625 was mounted in 1.680 refractive index oil. The technician noted that this oil had a brown discoloration (generally mounting oil has a clear color to it). This did not appear to affect the quality of the slides. A probable iron particle was photographed in this slide, and the photo is in Figure 12 below (reddish in color).

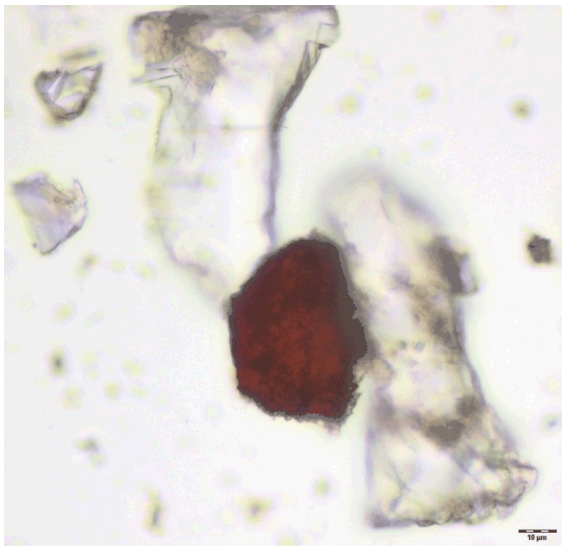

Figure 12. Sample S15R000625, Slide 3.

Uncrossed polars, reddish brown crystal in center is most likely an iron-containing compound.

Sample S15R000624 was a second split of sample 105C-15-03. This was the remainder of the grab sample that excluded the "white chunk" from above. Figure 13 below confirms the presence of dawsonite (blue circle) with some trona (red circle) and uranium particles also present (confirmed data from XRD analysis). Trace amounts of the isotropic crystal to the left of trona is sodium fluoride phosphate (white circle). S15R00624 appeared to have the highest presence of iron-containing compounds of any of the four samples analyzed (Figure 14).

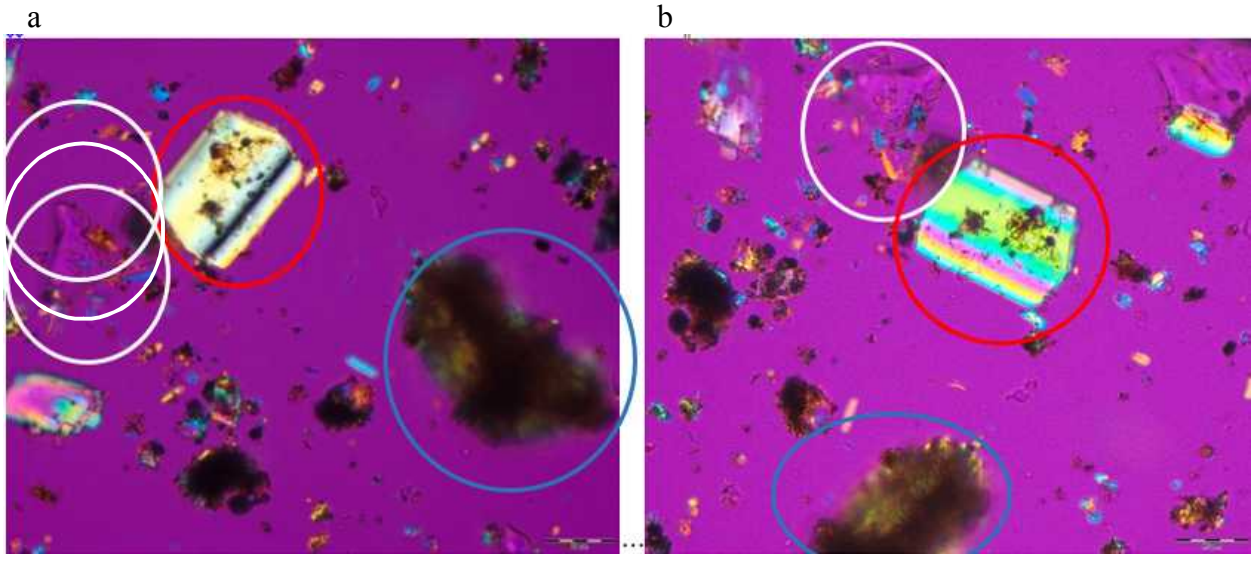

Figure 13. Sample S15R000624, Slide 1.

Red I compensator with crossed polars revealed characteristics of three identified particles in sample 105C-15-03. The two photos have been rotated 90 degrees from each other. Blue circle = dawsonite, Red circle = trona, and white circle = sodium fluoride phosphate.

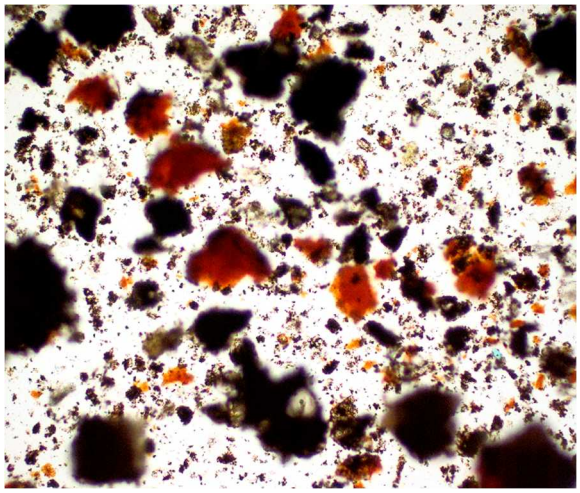

Figure 14. Sample S15R000624, Slide 1.

Uncrossed polars revealed the natural reddish color of iron-containing compounds in Sample 105C-15-03 where particles like the reddish ones in the figure above were most abundant.

Samples **S15R000622 and S15R000623** are subsamples of 105C-15-01 and 105C-15-02, respectively, and are very similar. The figures below illustrate the components observed in the samples. Major constituents include dawsonite (Figure 15), sodium carbonate/trona (Figure 17), and cejkaite (Figure 18). Unidentified phases in the photographs below include crystals with low birefringence (Figure 16) and the black substance that appears as coatings on crystals as well as singularly throughout the slides (Figure 17). When the sample was mounted in water, the most prevalent phases were dawsonite, cejkaite, and the unknown matter in Figure 16. In sample S15R000623 there was also sodium fluoride phosphate observed (Figure 15 (clear grain to right)) and iron-rich particles (Figure 19).

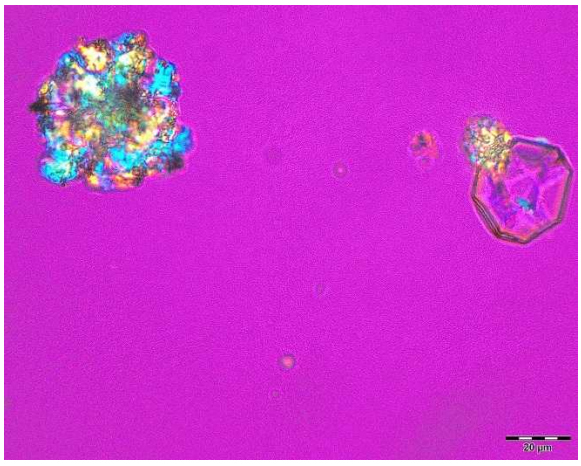

Figure 15. Sample S15R000623, Slide 1.

Dawsonite (left) and natrophosphate (right). Crossed polars with the Red I compensator.

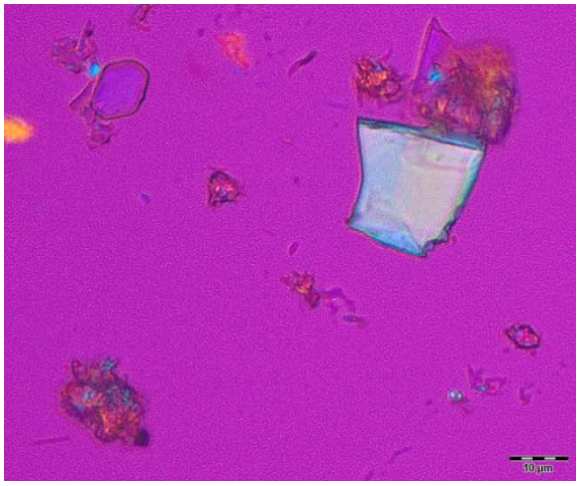

Figure 16. Sample S15R000622, Slide 3.

Unknown: low birefringence under crossed polars with the Red I compensator.

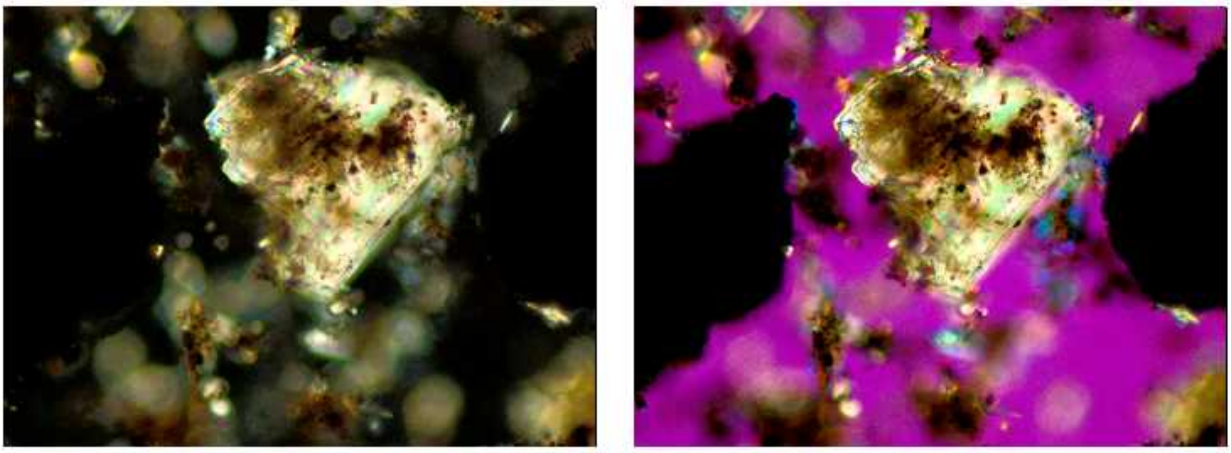

Figure 17. Sample S15R000622, Slide 1.

Suspect organic matter on this trona crystal. Crossed polars with and without the Red I Compensator.

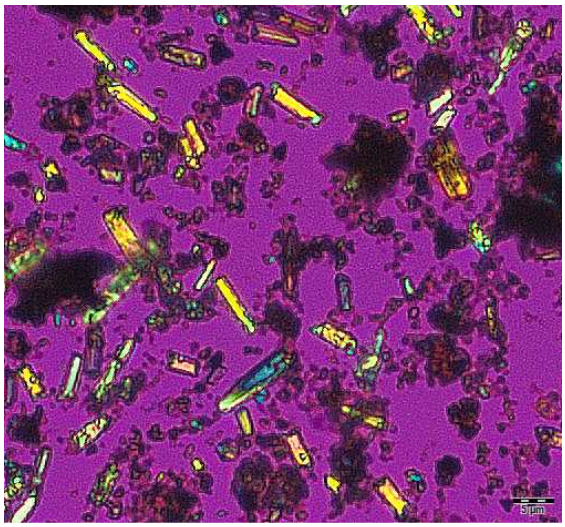

Figure 18. Sample S15R000622, Slide 2: Cejkaite Rods.

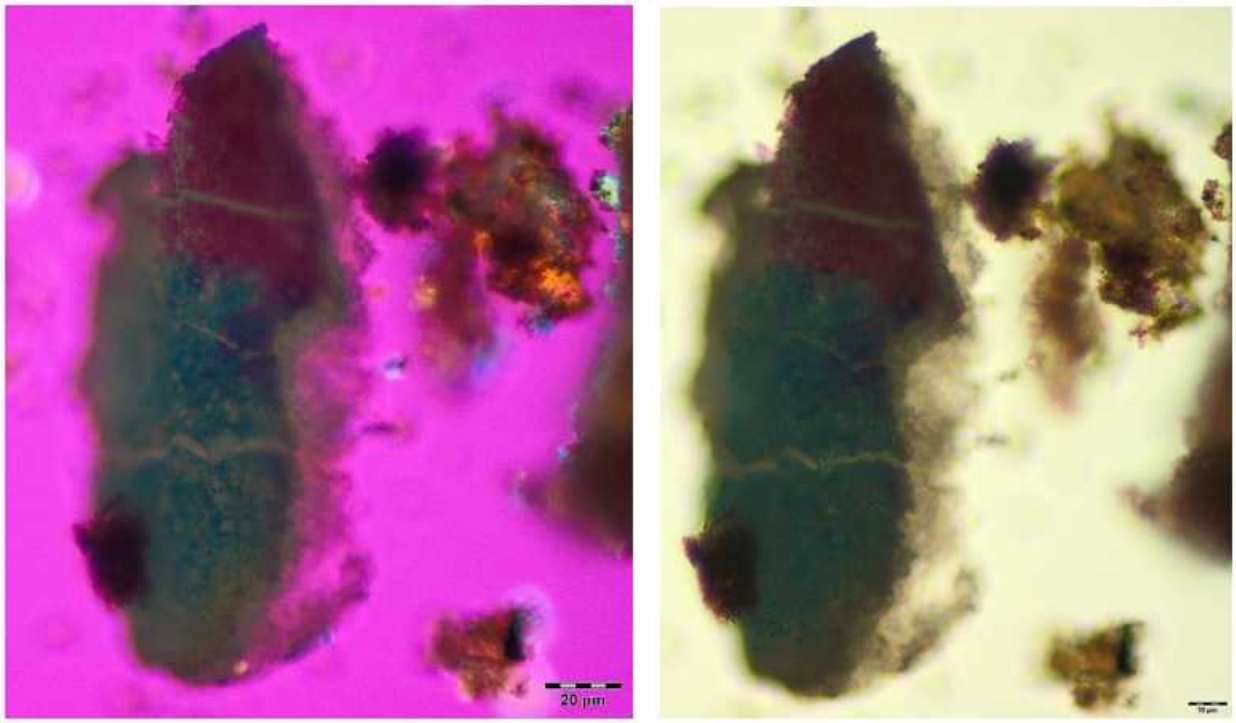

Figure 19. Sample S15R000623, Slide 3.

Oxidized iron particle (red/green color). Crossed polars with red I compensator and uncrossed polars without the red I compensator.

4 SCANNING ELECTRON MICROSCOPY

The samples are composed largely of sodium salts and a sodium-uranium-bearing particulate. The dominant sodium salt appears to be a mixture of sodium carbonate monohydrate

(thermonatrite) (Figure 20) and sodium carbonate bicarbonate (trona, $Na_3(CO_3)HCO_3$). Large, blocky sodium fluoride phosphate hydrate crystals (natrophosphate) are scattered throughout the samples (Figure 21) but represent a minor phase. Aluminum occurs mainly with sodium, in small aggregates of even smaller whisker-like crystals (Figure 22). This material, too tiny to resolve on the PLM, is likely dawsonite ($NaAl(OH)_2CO_3$) and represents a major phase, perhaps the dominant phase. Trace amounts of aluminum hydroxide (probably gibbsite) are also observed (Figure 23). In the light grains from 105C-15-03 (S15R000625), there was one small aggregate that was primarily aluminum-rich. But the majority of the hard tan aggregate is composed of sodium carbonate. Finally, there is a significant amount (estimated to be greater than 10%) of a sodium-uranium-rich phase in all samples. Many of these are in the form of hexagonal columns up to 50 microns long (Figure 24). These larger crystals were seen in the PLM analysis. The optical characteristics of this particulate are consistent with cejkaite, a sodium uranium carbonate, $Na_4(UO_2)(CO_3)_3$.

The images below are backscatter electron images, paired with the EDS chemical spectrum from the spot marked with the +.

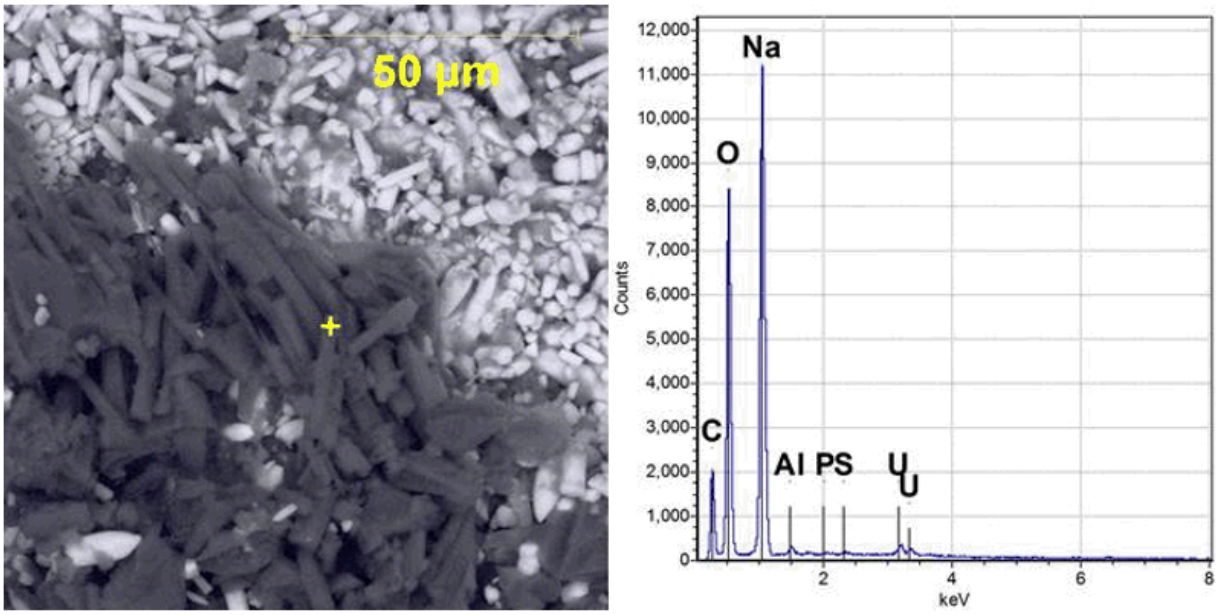

Figure 20. Sample 105C-15-01 (S15R000622): Thermonatrite and/or Trona.

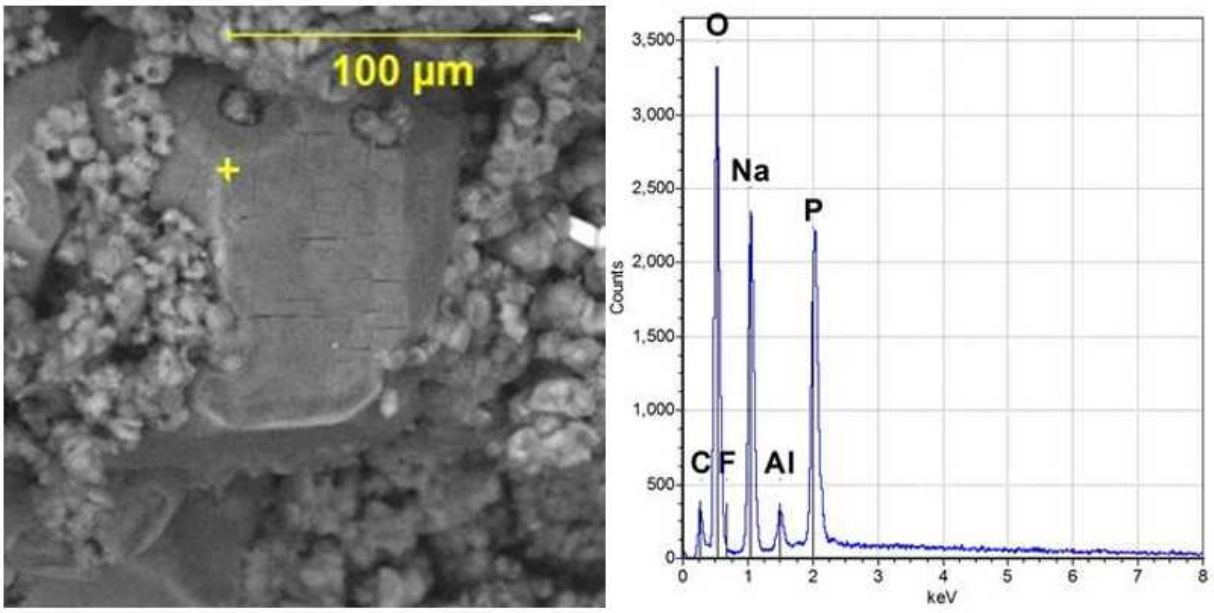

Figure 21. Sample 105C-15-03 (Dark Grains, S15R000624): Natrophosphate.

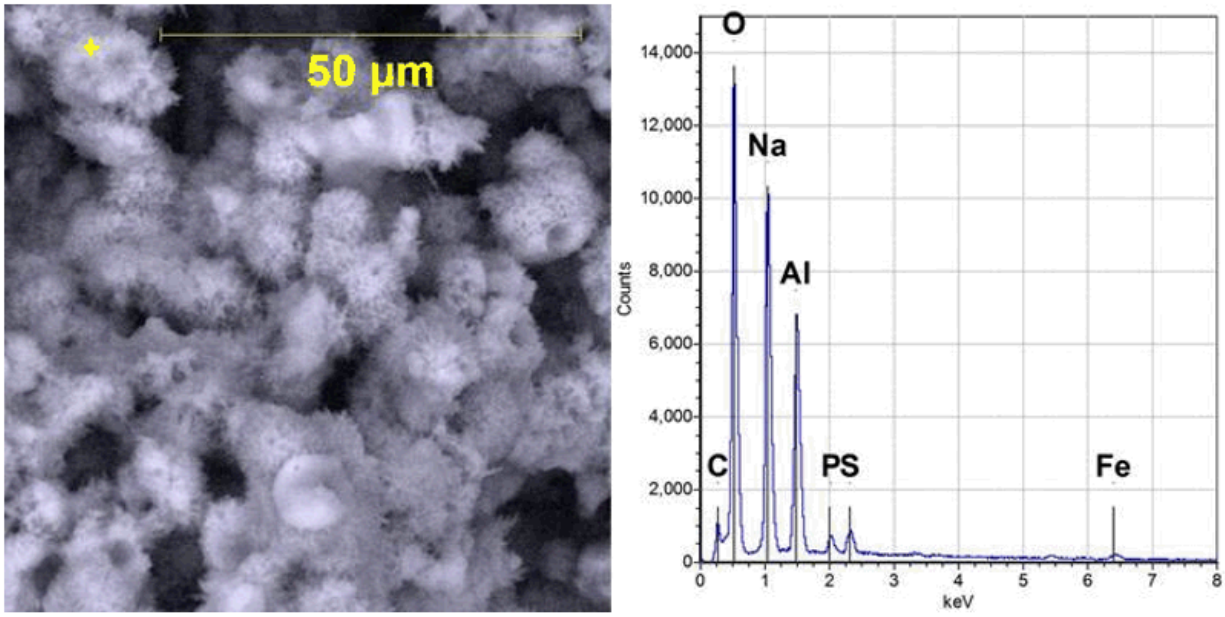

Figure 22. Sample 105C-15-03 (Dark Grains, S15R000624): Dawsonite.

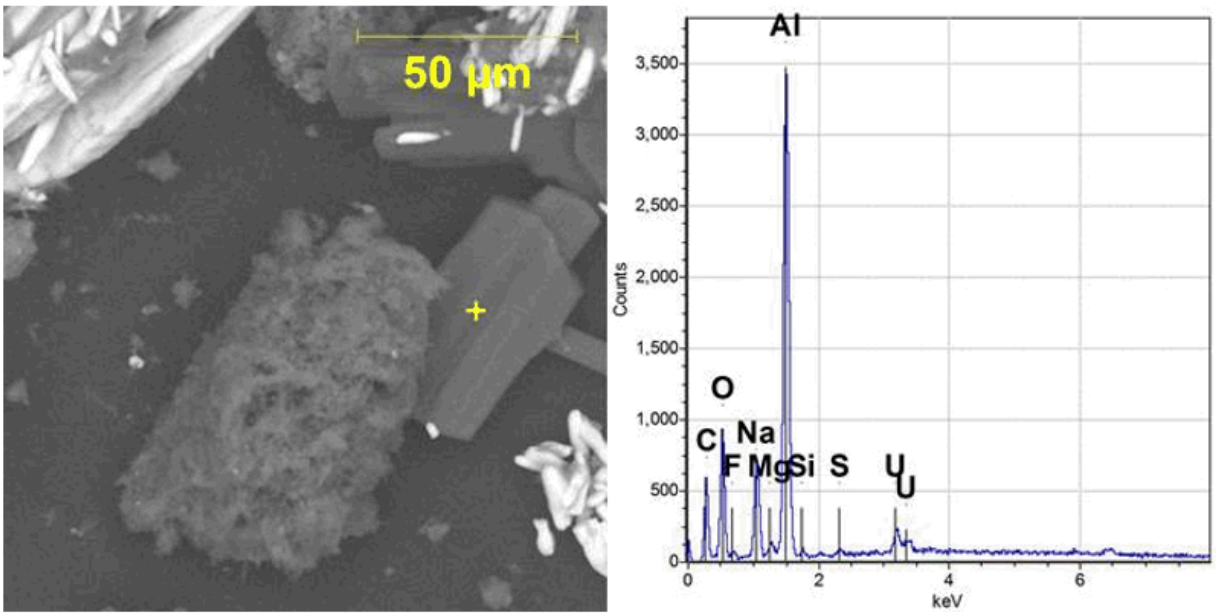

Figure 23. Sample 105C-15-01 (S15R000622): Gibbsite.

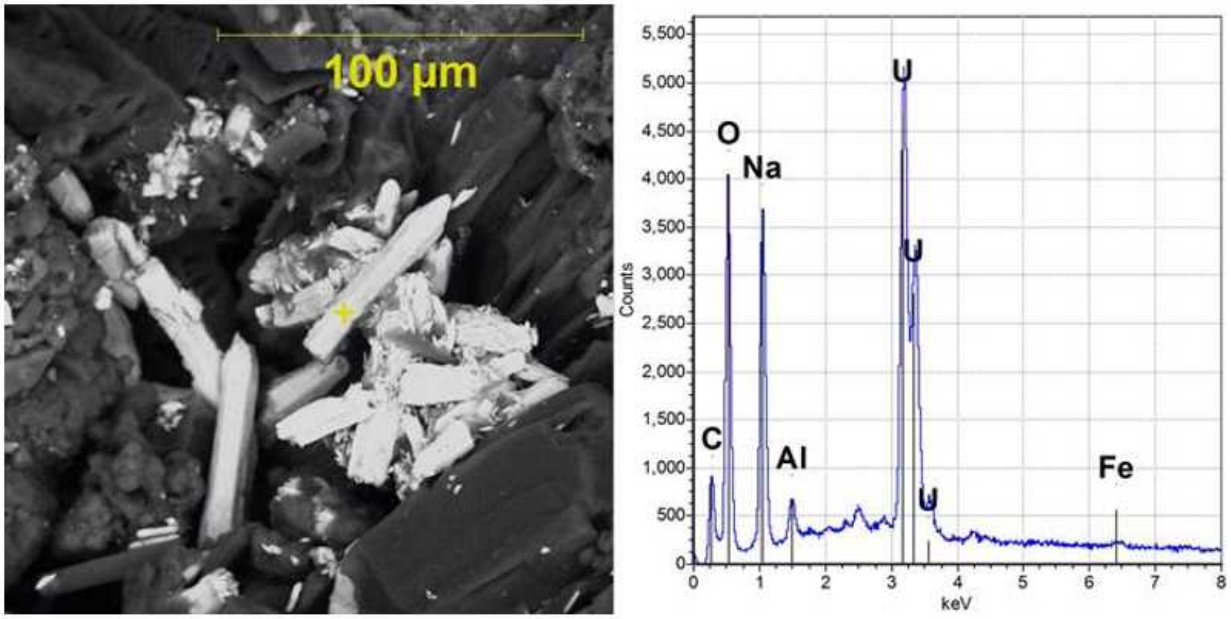

Figure 24. Sample 105C-15-03 (Light Grains, S15R000625): Cejkaite.

The presence of a carbon peak on all spectra suggests that the particulate may be coated with an organic phase. This could account for the static charge and flighty nature of the material. The material is generally quite inhomogeneous with patches and agglomerates of particle types varying widely across the surface of the SEM specimen and from one sample to the next.

However, all of the specimens analyzed had the same general characteristics described in this preliminary report.

5 DISCUSSION

Trona was found in the Tank 241-C-108 Heel samples (after retrieval to Tank 241-AN-106). This was confirmed by XRD and reported in LAB-RPT-10-00001, *Results of Physicochemical Characterization and Caustic Dissolution Tests on Tank 241-C-108 Heel Solids.* Attachment B to LAB-RPT-10-00001 contains the XRD patterns, and there are images on pages B-3 and B-5.

Dan Herting made trona by sparging Tank 241-AN-107 supernatant waste with CO_2. This is reported in 7S110-DLH-06-049, "Carbonation Test Results, Tank 241-AN-107." See page 8 and 9 in 7S110-DLH-06-049 for the discussion and figures.

Interestingly, trona was identified in the AW thermocouple wire efflorescence (WRPS-1501291, "Phase and Chemical Analysis of AW Thermocouple Wire Efflorescence"). The source of this trona was attributed to caustic that had not contacted tank waste interacting with nearby soils.

Cejkaite has only been reported in Tanks 241-C-203, 241-C-204, and 241-AN-106 (presumably) in PNNL-14903, Rev. 1, *Hanford Tanks 241-C-203 and 241-C-204: Residual Waste Contaminant Release Model and Supporting Data*. Note the morphology is similar to what we are seeing in C-105, and it is somewhat water soluble. Uranium crystals with morphology similar to those identified here as cejkaite have previously been seen in a Tank 241-C-108 sample, but not identified as such at the time of the report (LAB-RPT-10-00001, p. B-4).

In summary, the major phases identified in the C-105 grab samples (all 4 samples) and their anticipated solubility characteristics, in approximate order of abundance, are shown in Table 7.

Table 7. Summary of Solid Phase Characterization and Anticipated Solubility on C-105 Solid Samples.

Phase	**Estimated solubility in:**		
	H_2O	**19M NaOH**	**Nitric and/or oxalic acid**
Dawsonite	Insoluble	Readily soluble	Readily soluble
Thermonatrite and/or Trona	Soluble (given time)	Insoluble	Soluble (decomposes with gas evolution)
Cejkaite	Partially soluble (pH dependent)	Likely insoluble	Soluble (decomposes with gas evolution)
Natrophosphate	Soluble	Insoluble	Soluble
Unknown organic	Unknown, likely insoluble		
Trace phases (Fe-rich, gibbsite …)	Insoluble	Potentially soluble (Al phases)	Potentially soluble

6 REFERENCES

ATS-LT-161-103, 222-S Laboratory Technology Procedure for the ASPEX Explorer Scanning Electron Microscope, Revision A0, Washington River Protection Solutions LLC, Richland, Washington.

ATS-LT-161-104, SEM Sample Preparation Procedure, Revision A0, Washington River Protection Solutions LLC, Richland, Washington.

ATS-LT-507-103, "222-S Laboratory X-Ray Diffractometry (XRD) Using The Rigaku MiniFlex II," Revision C0, Washington River Protection Solutions LLC, Richland, Washington.

ATS-LT-519-107, "222-S Laboratory Polarized Light Microscopy, Revision G0, Washington River Protection Solutions LLC, Richland, Washington.

7S110-DLH-06-049, 2006, "Carbonation Test Results, Tank 241-AN-107," (internal memo from Analytical Process Development to K. G. Carothers, January 5), Washington River Protection Solutions LLC, Richland, Washington.

LAB-RPT-10-00001, 2010, *Results of Physicochemical Characterization and Caustic Dissolution Tests on Tank 241-C-108 Heel Solids*, Washington River Protection Solutions LLC, Richland, Washington.

LAB-RPT-12-00010, 2013, *Solid Phase Characterization of Tank 241-AY-102 Annulus Space Particulate*, Washington River Protection Solutions LLC, Richland, Washington.

PNNL-14903, 2004, *Hanford Tanks 241-C-203 and 241-C-204: Residual Waste Contaminant Release Model and Supporting Data*, Pacific Northwest National Laboratory, Richland, Washington.

WRPS-1501291, 2015, "Phase and Chemical Analysis of AW Thermocouple Wire Efflorescence," (internal memo from G. A. Cooke to A. M. Templeton, April 7), Washington River Protection Solutions LLC, Richland, Washington.

ICDD PDF 4+ data base, version 4.1504, International Center for Diffraction Data, 12 Campus Blvd., Newtown Square, PA 19073-3273 U.S.A.

Electronically Approved by:

UserName: Ely, Thomas (h4879082)
Title:
Date: Tuesday, 29 December 2015, 11:21 AM Pacific Time
Meaning: Approved by the author or delegate
==========

UserName: Lachut, James (h0062379)
Title:
Date: Wednesday, 30 December 2015, 02:40 PM Pacific Time
Meaning: Additional approval obtained
==========

UserName: Templeton, Andrew (h0091402)
Title: GEOLOGIST
Date: Tuesday, 05 January 2016, 08:12 AM Pacific Time
Meaning: Approved by the customer or delegate
==========

UserName: Cooke, Gary (h0410221)
Title: APD Chemist
Date: Thursday, 07 January 2016, 08:08 AM Pacific Time
Meaning: Approved by the Group Manager or delegate
==========